AFIT/GSO/ENG/93D-03

AD-A274 033

DTIC
S ELECTE
DEC 2 3 1993
A

SYSTEM DESIGN ANALYSIS OF A
LIGHTWEIGHT LASER SATELLITE TERMINAL

THESIS

Brian C. Page, Major, USAF

AFIT/GSO/ENG/93D-03

93-30926

93 12 22 030

# SYSTEM DESIGN ANALYSIS OF A

# LIGHTWEIGHT LASER SATELLITE TERMINAL

## THESIS

Presented to the Faculty of the Graduate School of Engineering

of the Air Force Institute of Technology

Air University

In Partial Fulfillment of the

Requirements for the Degree of

Master of Science in Space Operations

| Accesion For | |
|---|---|
| NTIS CRA&I | ☑ |
| DTIC TAB | ☐ |
| Unannounced | ☐ |
| Justification | |

| By | |
|---|---|
| Distribution / | |

| Availability Codes |
|---|

| Dist | Avail and/or Special |
|---|---|
| A-1 | |

Brian C. Page, B.S.

Major, USAF

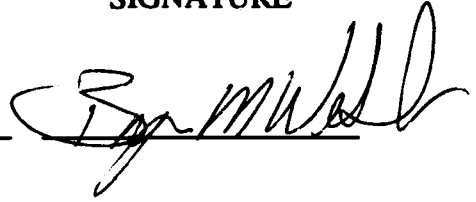DECEMBER 1993
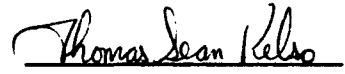
DTIC QUALITY INSPECTED 3

# THESIS APPROVAL

STUDENT: Brian C. Page          CLASS: GSO 93D

THESIS TITLE: SYSTEM DESIGN ANALYSIS OF A

LIGHTWEIGHT SATELLITE TERMINAL

DEFENSE DATE: 17 Nov 93

| COMMITTEE: | NAME/DEPARTMENT | SIGNATURE |
|---|---|---|
| Co-Advisor | Byron M. Welsh / ENG | |
| Co-Advisor | Michael C. Roggemann / ENP | |
| ENS Representative/Reader | Thomas S. Kelso / ENS | |

# Preface

The purpose of this study was to determine if technological advancements have progressed enough to make a man-portable satellite laser communications system feasible. To determine this feasibility three objectives were accomplished: an end-to-end system analysis on the communications link; evaluation of atmospheric effects; and evaluation of semi-conductor lasers as the laser source.

Baseline satellite communication systems were analyzed for both conventional radio frequency systems and a laser communication system. Modifications to the laser communications system were explored, and found to be feasible for some applications. Atmospheric effects were explored and are a major contributor to system degradation. Semiconductor laser sources were evaluated and are currently useful for some satellite laser communication applications.

I received an enormous amount of help from numerous people. I am deeply indebted to both my faculty advisors, Capt. M. C. Roggemann and Dr. B. M. Welsh for their undying patience and guidance. I would like to thank McDonnell Douglas Aerospace, in particularly Doug Dreisewerd who provided material from their research efforts and answered questions at a level I could understand. Additionally both Sandi Weaver and Jim Chetwynd contributed vast amounts of their help in getting access to the LOWTRAN and FASCOD atmospheric models. Finally, I wish to thank my wife Susan and my three daughters for their understanding during all the evenings and weekends I worked on this thesis and could not devote that time to them.

Brian C. Page

# Table of Contents

# List of Figures

# List of Tables

AFIT/GSO/ENG/93D-03

# Abstract

This study investigated the technological feasibility of a man-portable satellite laser communications system. Areas of interest were: an end-to-end system analysis on the communications link; evaluation of atmospheric effects; and evaluation of semi-conductor lasers as the laser source. A literature search revealed that satellite laser communication research is primarily directed at inter-satellite links. There have been some proposed systems for space-to-ground laser communications systems, but they all utilize large fixed ground stations. The focus of this research effort is directed at a small man-portable ground station capitalizing on recent advances in semiconductor laser devices.

Baseline satellite communication systems were analyzed for both conventional radio frequency systems and a laser communication system. Modifications to the laser communications system were explored, and found to be feasible for some applications. Atmospheric effects were explored and are a major contributor to system degradation. Semiconductor laser sources were evaluated and are currently useful for some satellite laser communication applications.

# SYSTEM DESIGN ANALYSIS OF A
# LIGHTWEIGHT LASER SATELLITE TERMINAL

## I. Introduction

As shown in Desert Storm, military forces are increasingly using lightweight satellite terminals to communicate. These terminals are carried in the backpacks of ground patrols, mounted on jeeps, and carried aboard ships and aircraft. Operators such as Special Operations troops, often rely on these portable terminals to communicate with their headquarters or base camps. They pass on enemy locations, troop movements, and infill/exfill instructions, to name but a few of the multitude of uses. The nature of their often covert mission requires them to remain undetected while behind enemy lines and hopefully maintain reliable unjammed communications.

Conventional terminals utilize radio frequency (RF) bands and can be limited in several ways: low data transmission rates (1200 to 2400 bps); high probability of intercept (wide antenna patterns 65° to 90°); and susceptibility to jamming (13:1; 15:1). The low data transmission rates are fine for some applications, but for transmission of maps and reconnaissance photographs a high data rate is desirable, if not mandatory, to reduce the transmit and receive times, and thus exposure of covert operating locations. The wide antenna pattern causes increased probability of intercept as Figure 1.1 shows. Both ground units and airborne sensors can intercept this wide pattern. Once intercepted, the
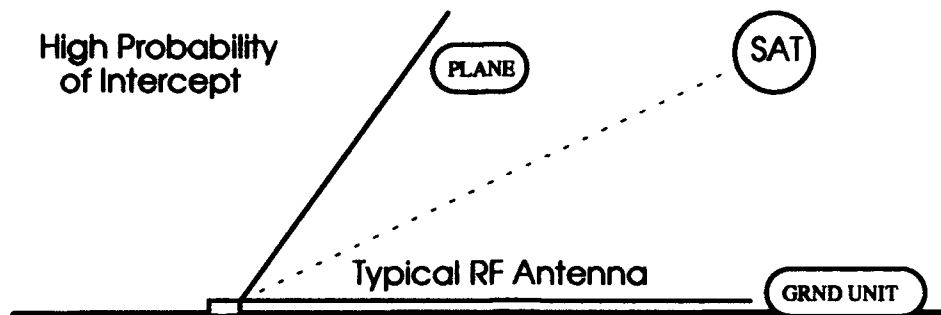
**Figure 1.1  RF Beam Pattern and Probability of Intercept**

operator's position can be determined, and jamming can ensue.  Both effects are detrimental to covert operations.  Current technology offers a possible solution to these inherent problems: *laser communications*.

Laser communications (lasercom) offer very high data rates (multi-giga bps), low probability of intercept (very narrow antenna patterns - microradians or $10^{-5}$ degrees), and low susceptibility to jamming (6:1163).  Figure 1.2 shows how laser antenna patterns are much less prone to interception and jamming due to their very narrow nature.
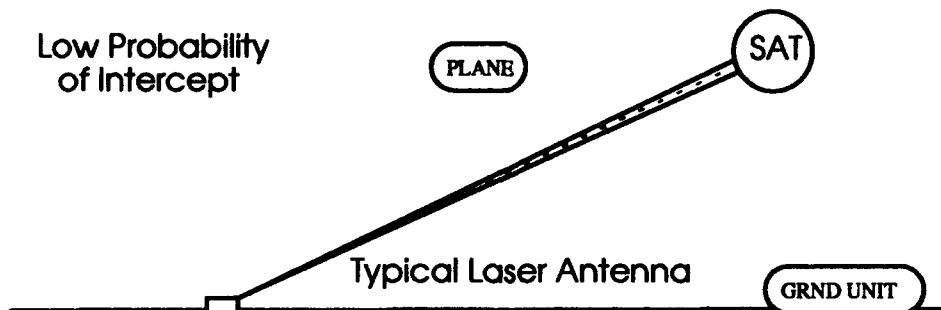


**Figure 1.2  Laser Beam Pattern and Probability of Intercept**

The concept is simple: use lasercom to take advantage of high data rates and narrow beam patterns.  So why don't we currently use portable lasercom units for ground-to-satellite communication systems?  The answer historically comes in two parts: weather and physical attributes.

Weather typically includes clouds, rain, and other atmospheric or man-made phenomena (such as dense smoke as seen in Desert Storm) which cause drastic reduction in lasercom performance. These factors can make the difference in a successful or failed lasercom link. Although research is ongoing to mitigate these weather factors, and is promising at least for low-data-rate lasercom (naval submarine communications), it is beyond the scope of this thesis.

Physical attributes include such factors as size, weight, and power consumption. Historically, lasers started out the size of table tops, weighing tens to hundreds of pounds, and consuming tens to hundreds of watts (ruby rod, $CO_2$, NdYAG). These physical attributes would obviously not be conducive to either ground-portable units or satellite units. Research and development (R&D) in this area has significantly improved these factors. Has this R&D effort improved lasercom to the point where it is feasible for portable ground-to-satellite lasercom systems? Therein lies the problem for this thesis.

## Problem

Do we have the technology to develop a field transportable satellite laser communications system which has:

- High data rate (Mbps to Gbps)
- Low probability of intercept (LPI)
- Jam resistant

## Objectives

The objectives of this thesis will be to:

- Accomplish an end-to-end system design analysis on the communications link
- Evaluate atmospheric effects
- Evaluate semiconductor lasers as the laser source

1-3

The end-to-end system design analysis will pursue a satellite lasercom system which will take advantage of high data rates, be lightweight, have small power consumption, and be small in size. The system will have two terminals: 1) the ground terminal; 2) the geosynchronous (GEO) satellite terminal. The ground terminal should be as small and lightweight as possible to allow it to be man-portable; so a man can carry it in a backpack. This in turn demands the power consumption be small, because it will have to operate on a battery. The satellite terminal can be larger than the ground terminal, but only to the extent that it must fit on a satellite bus, that it is limited to the size and weight restrictions of launch, and that its power consumption is limited to the power available from the satellite (assumed to be solar panels). Evaluation of atmospheric effects will include atmospheric absorption, atmospheric scintillation, and aperture averaging. Evaluation of semiconductor lasers will include current commercially available lasers, as the laser source for both the ground terminal, and the GEO terminal.

## Previous Work

Several past efforts address satellite lasercom systems or related technical demonstrations. These include an Air Force aircraft-to-ground lasercom experiment from 1977 - 1980, a TRW analysis of laser uplinks and downlinks in 1988, and a series of analyses by McDonnell Douglas on satellite laser crosslink designs between 1992 - 1993. Each of these efforts contribute substantially to an overall satellite-to-ground lasercom system, but none specifically address a man-portable ground terminal.

The Air Force's Laser Communications Airborne Flight Test System (AFTS) experiment contributed substantially to our understanding of atmospheric effects on lasercom, and demonstrated that 1 Gbps links could be accomplished. The experiment was conducted at slant ranges up to 100 km and at a slant angle (7°) much more severe than most ground-to-satellite lasercom systems will operate (6:1167). For our purposes,

the AFTS experiment proved 1Gbps lasercom is viable in worst case (slant angle and range) atmospheric conditions. Additionally, AFTS successfully demonstrated several other objectives: 1) narrow-beam lasers can successfully be used for acquisition and tracking; 2) quadrant avalanche photodiodes (APD) have the accuracy, stability, and sensitivity needed for acquisition and tracking (9:57-64).

TRW's work analyzes geosynchronous-to-airplane or geosynchronous-to-ground up/downlinks. Atmospheric effects are discussed and evaluated. Use of coding to mitigate atmospheric losses and mention of several methods to minimize susceptibility to jamming are notable. The geosynchronous-to-ground downlink utilizes a 39-inch diameter receiver located 20 meters above the ground (atop a six-story building), which is beyond the practical size, weight, and operating limitations of a man-portable ground terminal. (2:65-71)

McDonnell Douglas has done extensive work in the satellite crosslink field. Notable is their crosslink equipment. They are currently developing a seventh-generation crosslink which utilizes dichroic combination of thermally-tuned semiconductor lasers. Their use of gimbaled Gregorian telescopes, application-specific integrated circuits (ASICs), and high-powered laser diodes, make these multi-giga bps lasercom crosslink terminals a good choice for lightweight and reliable space-borne satellite terminals. Additionally, McDonnell Douglas accomplished an analysis on satellite-to-ground up/downlinks, to include an in-depth look at atmospheric effects. Their ground terminal utilizes a large aperture (36-inch diameter) which is not practical for a man-portable ground terminal. (9:225-235; 10; 11:183-187; 12:1163-1169; 13:177-182; 14:1-11)

# II. Methodology

In order to analyze a laser communications (lasercom) system the basic equations, computer models, and theory must be explored. Once these basic tools are understood, a baseline system can be designed and analyzed. Parameters in this baseline system can then be varied, such as laser power and beamwidth to contrast effects of different system components. Additionally, a comparison between lasercom systems and current RF satellite communications (satcom) systems will be useful.

The comparison between the RF and laser satcom systems will be made in the Results and Conclusion chapters. The tools required to analyze an RF satcom system are well developed, as evidenced by the myriad of RF communication satellites in orbit. Appendix A reviews an RF satcom system. The remainder of this chapter deals with tools required to analyze a lasercom system.

## Link Margin Equation

The link margin equation is the basic tool which establishes system performance parameters and measures. The link equation is a means of calculating the required signal levels with respect to gains and losses in the entire system. The system primarily includes the transmitter, the link path, and the receiver. The link equation specifically calculates the ratio (signal margin) of detected signal energy to the signal energy required for a specified performance level. Performance level for a digital communications system can be based on the probability of bit error ($P_e$). Equation (2-1), gives the link equation. The terms in Equation (2-1) are in dB, to allow for ease of computation. The individual terms of the equation will be explored further in the sections to follow. (28:13)

2-1

$$M = P + G_T + \tau_{txopt} + \eta_{ff} + L_n + FSL + \tau_{atm}$$
$$+ FM + G_R + \tau_{rxopt} + \eta_{dd} - S_{REQ} \tag{2-1}$$

where

| | | |
|---|---|---|
| $M$ | = | Link margin (dB) |
| $P$ | = | laser output power (dBW) |
| $G_T$ | = | transmit antenna (telescope) gain (dB) |
| $\tau_{txopt}$ | = | transmit antenna optics transmissivity (dB) |
| $\eta_{ff}$ | = | far field on-axis efficiency (dB) |
| $L_n$ | = | transmit antenna wavefront efficiency (dB) |
| $FSL$ | = | free space propagation loss (dB) |
| $\tau_{atm}$ | = | atmospheric losses: molecular absorption |
| $FM$ | = | atmospheric scintillation and aperture averaging (dB) |
| $G_R$ | = | receiver antenna gain (dB) |
| $\tau_{rxopt}$ | = | receiver antenna optics transmissivity (dB) |
| $\eta_{dd}$ | = | direct detection receiver efficiency |
| $S_{req}$ | = | signal required for minimum performance based on detector noises, quantum efficiency, and gain |

The link margin $M$ is the ratio of the actual signal energy to the required signal energy.

## Transmitter

The transmitter encompasses the laser source, the modulation technique, and the optics. Each of these terms are interrelated which creates a challenge for the system designer.

**Laser Power.** The power $P$ in the link margin equation is based on peak laser power $P_{pk}$:

$$P = 10 \log(P_{pk}) \tag{2-2}$$

In order to calculate the peak laser power, the basic power relationship must be understood, as well as the type of modulation, the data rate in bits per second (bps), and the resulting pulse width and pulse repetition rate. The basic power relationship can be related using the following equation:

$$P_{avg} = P_{pk} \times PW \times PRR \tag{2-3}$$

where

$P_{avg}$ = average output power of a laser (W)

$P_{pk}$ = peak power of the laser pulse (W)

$PW$ = pulse width (sec)

$PRR$ = pulse repetition rate (pps)

The modulation type determines the number of information bits per pulse, and the data rate will, inturn, drive the pulse width and pulse repetition rate. For instance, a Manchester modulation type with a 50 percent duty cycle and a 1-Gbps data rate requirement, requires binary, 1 bit per pulse, 500 psec pulse widths, at 1 Gpps.

For a CW semiconductor laser with an average rated output power $P_{avg}$ that is pulsed via current modulation, the peak power $P_{pk}$ of a pulse is approximately equal to this average rated power given in the laser specifications. This assumes the laser can respond fast enough to reach the full power ($P_{avg}$) in the given pulsewidth time frame.

**Transmitter Antenna Gain.** The transmitter antenna gain is the ratio of the radiation intensity from the antenna, to the radiation intensity of an ideal isotropic radiator driven by the same input power (28:22). For a refractive type telescope, on axis transmitter gain $G_T$ can be calculated by using the full width $1/e^2$ maximum beam divergence angle $\theta_t$ (28:23):

$$G_T = 10 \log_{10} \frac{32}{\theta_t^2} \qquad (2\text{-}4)$$

**Beamwidth.** The optimum beam divergence angle (beamwidth) $\theta_t$ can be calculated based on several methods. In general, $\theta_t$ is related to the required minimum pointing error $\theta_\epsilon$ (28:50):

$$\theta_t \cong 2.838\,\theta_\epsilon \qquad (2\text{-}5)$$

However, for lasercom systems that propagate through the atmosphere, the beamwidth has to be related to beamsteering effects caused by the fluctuating path the signal takes through atmosphere. The path fluctuates in angle due to the changes in index of refraction caused by temperature differences from one layer of the atmosphere to another. Additionally, the wind causes the temperature in these layers to fluctuate, which, inturn, causes a temporal fluctuation in the index of refraction. If the beamwidth is too narrow, these fluctuations in the index of refraction manifest enough atmospheric beamsteering to cause the target system to be completely missed. Figure 2.1 shows this. This figure also shows that the beamsteering effects are more severe for an uplink, since the atmosphere affects the laser signal at the beginning of its path (shower door effect). (12:1166)
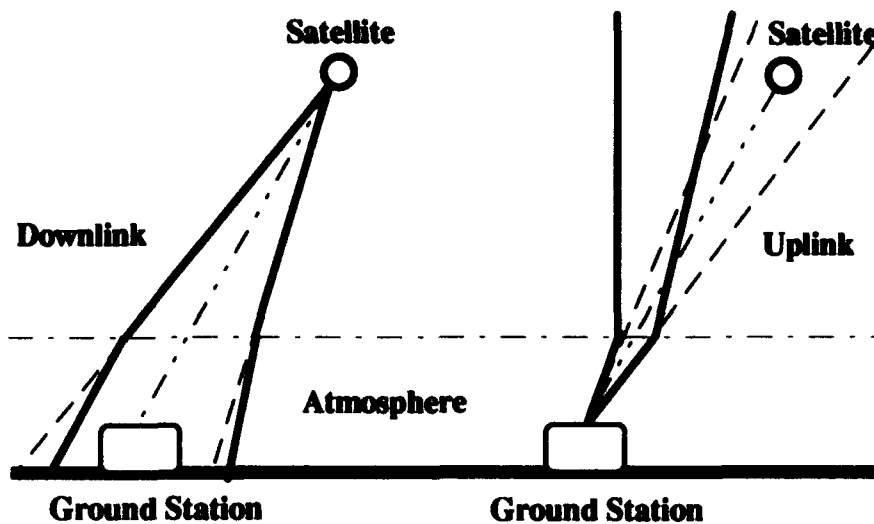
**Figure 2.1 Beamsteering Effects** (12:1166)

Thus, in order to calculate the beamwidth, the atmospheric winds and the changes in index of refraction must be modeled first.

**Wind Model.** The atmospheric wind can be modeled based on the probabilistic nature of the wind with peaks in the wind speeds at the troposphere and stratosphere (31:I.4). Hufnagel has done this, and he bases his model on the following expression of wind speed $W(h)$ based on a particular altitude or height $h$ of interest (31:I.4-I.5):

$$W(h) = W_T \exp\left[-0.5\left(\frac{hP_T}{S_T/2}\right)^2\right] + W_S \exp\left[-0.5\left(\frac{hP_S}{S_S/2}\right)^2\right] \qquad (2\text{-}6)$$

where

$W(h)$ = wind speed at an altitude $h$ (m/sec)

$W_T$ = peak tropospheric wind = $-0.2776\,X^2 - 11.9553X + 36.4416$ (m/sec)

$W_S$ = peak stratospheric wind = $-0.5304\,X^2 - 18.3192X + 76.2704$ (m/sec)

$X$ = ln (-ln($P$))

2-5

$P$ = probability of occurrence

$S_T$ = tropospheric wind spread = $1000\left[\dfrac{W_T + 128.15}{18.3}\right]$ (m)

$S_S$ = stratospheric wind spread = $1000\left[\dfrac{W_s + 148.74}{6.65}\right]$ (m)

$P_T$ = height of maximum tropospheric wind = $11.88 \times 10^3$ (m)

$P_S$ = height of maximum stratospheric wind = $60 \times 10^3$ (m)

$h$ = altitude (m)

Figure 2.2 shows a plot of the wind speed versus altitude for a 0.95 probability of occurrence.
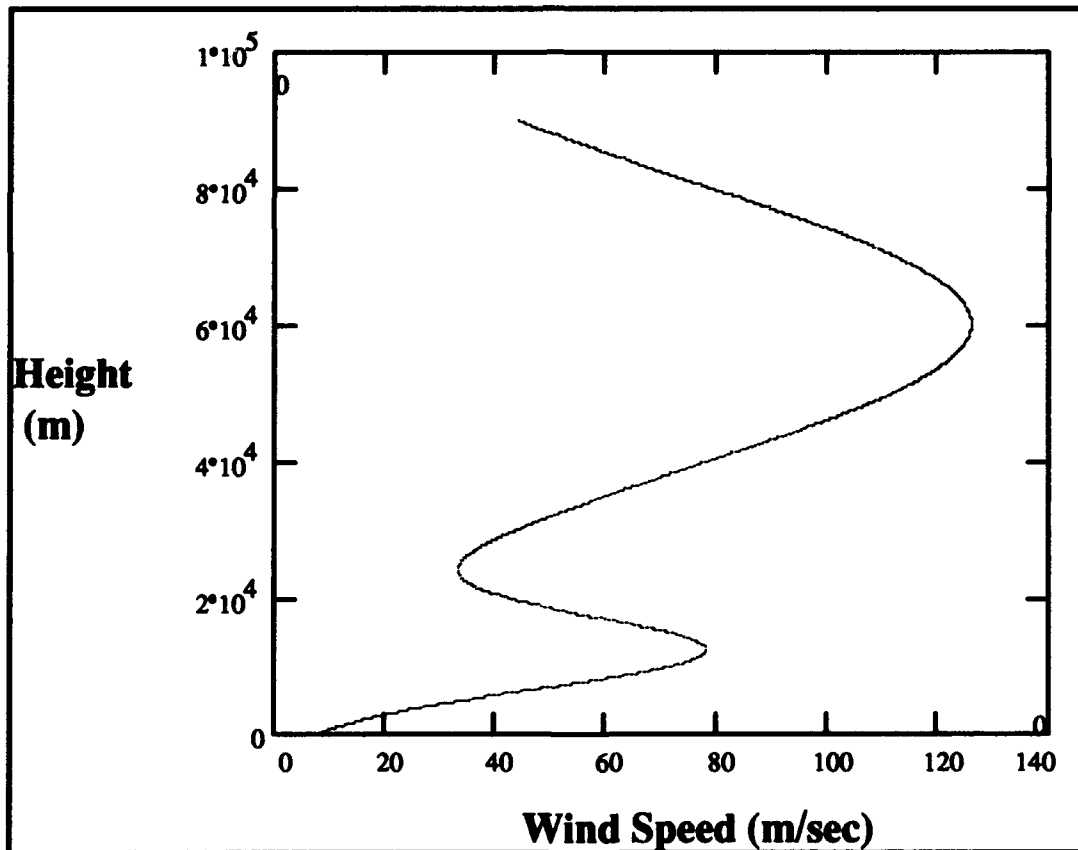


Figure 2.2  Hufnagel Wind Model

2-6

**Structure Constant.** From the wind model the changes in the index of refraction can be modeled. The structure constant $C_n^2(h)$ is used to describe the strength of the index of refraction fluctuations as a function of height $h$ (31:I.4-I.5):

$$C_n^2(h) = \left(C_{no}^2 - A\right)\exp\left[\frac{-h}{H_o}\right] + A\left(1 + \frac{W(h)^2}{C}\right)\exp\left[\frac{-h}{B}\right] \qquad (2\text{-}7)$$

where

$C_n^2(h)$ = structure constant at altitude $h$   ($m^{-2/3}$)

$A$ = $5.62 \times 10^{-19}$

$B$ = $4825$

$C$ = $16.49$

and the surface condition constants $C_{no}^2$ and $H_o$ are (31:I.4-I.5):

| | $C_{no}^2$ | $H_o$ |
|---|---|---|
| Sunny Day | $3.6 \times 10^{-13}$ | 261 |
| Clear Night | $1.6 \times 10^{-13}$ | 281 |
| Dawn/Dusk | $8.7 \times 10^{-15}$ | 388 |

The structure constant $C_n^2(h)$ can be depicted graphically as a function of height $h$. Figure 2.3 depicts the structure constant versus altitude for sunny day conditions.
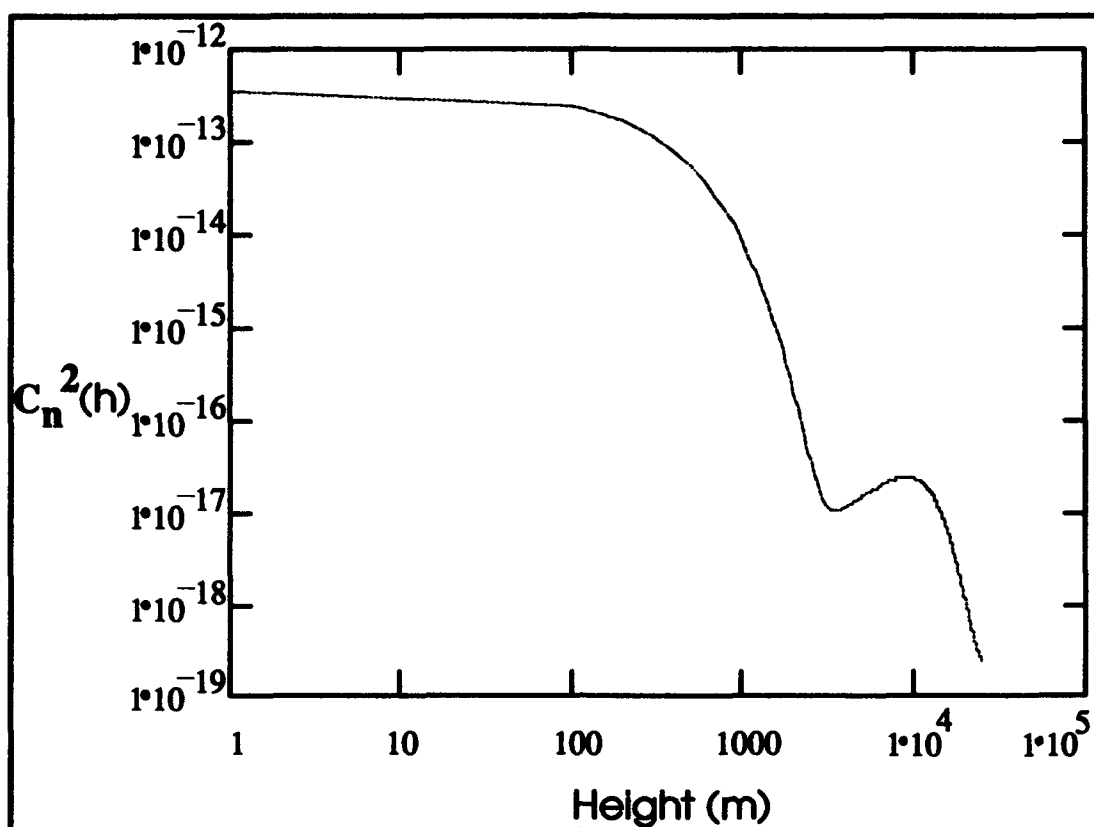
**Figure 2.3  Structure Constant**

The structure constant $C_n^2(h)$ can now be used to calculate the $1/e^2$ beamwidth $\theta_t$

from the following equations (31:I.12):

$$\theta_t^2 = \frac{128}{(kD_{ap})^2} + \frac{128}{(k\rho_0)^2}$$

(2-8)

where

$$k \quad = \quad \text{wavenumber} = \frac{2\pi}{\lambda}$$

$$\lambda \quad = \quad \text{wavelength (m)}$$

$$D_{ap} \quad = \quad \text{aperture diameter (m)}$$

and $\rho_0$ the spherical coherence length is (31:I.12):

$$\rho_0 = \left[1.45k^2 \int_0^R C_n^2(h)\left(1-\frac{h}{R}\right)^{\frac{5}{3}}\right]^{-\frac{3}{5}} \qquad (2\text{-}9)$$

where $R$ is the range or path distance in meters.

**Transmit Optics Transmissivity.** The transmitter optics is composed of filters, lenses (or mirrors), and any other optical elements required for the system. All these elements must be impedance matched and optimized to the wavelengths used. This matching is usually done via coatings on the elements. Individual transmissivities, $\tau$, are usually on the order of 99 percent and are multiplied together to get the total system transmissivity. Typical total system transmissivities range from 65 percent to 75 percent due to the amount of elements involved in the optical path. Total system transmissivity is annotated as $\tau_{txopt}$.

**Far Field On-Axis Efficiency.** The transmitter system has an additional loss due to the effects of diffraction on the far-field laser pattern. This loss can be put into terms of  far-field on-axis efficiency $\eta_{ff}$. The maximum $\eta_{ff}$ occurs when the $1/e^2$ laser beamwidth is not fully expanded to illuminate the full aperture size. Figure 2.4 shows that a maximum efficiency of 81 percent occurs when the aperture radius $a$ is 1.12 times larger than the $1/e^2$ beamwidth $\omega$. (28:185; 29:2134)
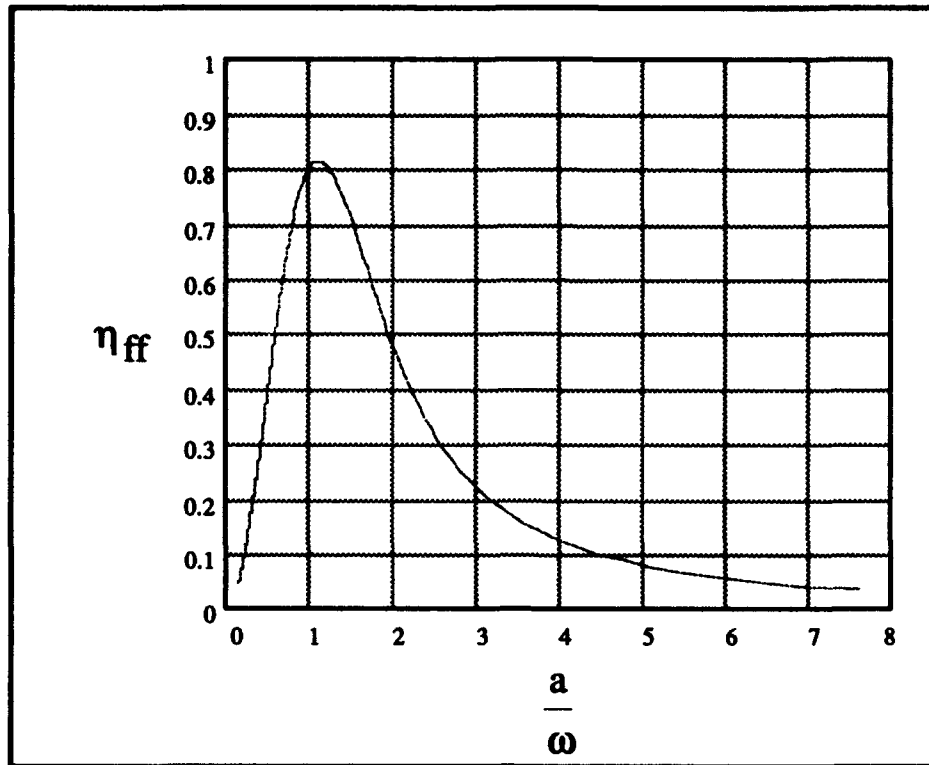
**Figure 2.4 Far Field On-Axis Transmitter Efficiency**

**Transmitter Antenna Wavefront Efficiency.** Wavefront quality is a primary factor determining antenna efficiency. Wavefront quality is a function of how well the optical surfaces are machined to tolerances, normally within 1 percent of the wavelength. The tolerances involved become the primary limitation of telescopes. Wavefront error causes the energy in the central lobe to broaden the far-field pattern and reduce the flux density. This ultimately causes a reduction in antenna gain. Strehl ratio is the measure of this degradation: the ratio of on-axis gain with wavefront error, compared to on-axis gain without wavefront error (28:26). The transmit antenna wavefront efficiency $L_n$ can be calculated from the Strehl ratio (28:26):

$$L_n = 10\log_{10}(Strehl\ ratio) = 10\log_{10}\exp\left[-(2\pi N/\lambda)^2\right] \qquad (2\text{-}10)$$

where N = number of waves of rms phase error across the aperture (N < 0.3 $\lambda$).

2-10

## Link Path

The link path includes everything between the transmitter and receiver. Primarily this includes free space loss, atmospheric absorption, atmospheric scintillation, and aperture averaging. The link path represents the major source of signal loss and noise source for the system.

**Free Space Loss.** Free space loss, *FSL*, refers to the propagation loss in free space, as the electromagnetic wave travels and spreads out with range (distance traveled). It is the largest loss in the link equation, and can normally be several hundred dBs for the distances involved in a ground-to-geosynchronous system. It can be calculated by using the link range, *R*, between transmitter and receiver (28:27):

$$FSL = 10\log_{10}\left(\frac{4\pi R}{\lambda}\right)^2 \tag{2-11}$$

**Atmospheric Absorption.** As a signal passes through the atmosphere the molecular and aerosol structure causes absorption and scattering, which, in turn, drives the overall atmospheric transmissivity to a lower value (22:1). This absorption is highly dependent on wavelength and can vary dramatically from one laser line (wavelength) to another. This places a premium on the choice of laser type and, thus, wavelength used. For instance, a $CO_2$ laser at 10.6 $\mu$m wavelength (944 cm$^{-1}$) has an atmospheric transmissivity of 87 percent when an AlGaAs semiconductor laser at 801 nm wavelength (1248 cm$^{-1}$) has only a 57 percent transmissivity (8:33). This also means that with a lasercom system which utilizes several laser lines spaced closely together (10 - 20 angstroms) to form a laser pulse, one or more of these laser lines may be substantially absorbed while others may pass through the atmosphere relatively unscathed.

This suggests that selection of a laser type and wavelengths requires a line-by-line inspection of atmospheric absorption in the regimes being considered. Typically,

atmospheric models such as LOWTRAN have been used to find atmospheric "windows" to operate in. PCTRAN7/LOWTRAN7 is the current version developed by Ontar Corporation and the U. S. Air Force Geophysics Laboratory. However, LOWTRAN7 only has a 20 cm$^{-1}$ resolution, which, in essence, does not give a capability to do line-by-line calculations. This means the program averages values over 20 cm$^{-1}$ wavenumbers and may not readily detect subtle changes. For example, LOWTRAN7 calculates an 87 percent transmittance for 10.6 $\mu$m, whereas a line-by-line calculation (FASCOD discussed below) for the same case gives a 32 percent transmittance (8:33). LOWTRAN7 will, however, provide complex geometry radiance calculations which will be utilized for background noise calculations (in later sections) which do not require line-by-line resolution. (4; 8:32-34; 36:1; 37:3.1-3.13; 38; 49)

A high spectral resolution line-by-line atmospheric model which utilizes the 1992 HITRAN database is available from Ontar/USAF Geophysics Lab: FASCOD3P. FASCOD3P offers an atmospheric model with 28 molecular species, numerous aerosol models, multiple scattering, ground/target reflectance, solar/lunar sources, as well as many other features which allow complex geometry absorption, transmittance, radiance, and irradiance calculations. FASCOD3P will be utilized for atmospheric loss $\tau_{atm}$ calculations. (3:1-8; 4; 8:33-34; 36:1; 37:3.1-3.13; 38; 49)

**Atmospheric Scintillation.** Scintillation is the constructive and destructive interference of the laser signal (optical wave) as it passes through regions of atmosphere with different indices of refraction. As in the previous section, the structure constant $C_n^2(h)$ is a measure of this change in the index of refraction, and can be used to calculate the variance, $\sigma_\chi^2$, of a signal due to atmospheric scintillation (5:1982-1994; 19:169-175; 20:175-180; 21:181-185; 22:1-3; 31:I.2-I.4; 42:341-351; 52:6.6-6.24; 55:1608-1609). Hinrichs has modeled this signal variance, $\sigma_\chi^2$, for a point receiver (31:I.8-I.10):

$$\sigma_\chi^2 = 0.563 \left(\frac{2\pi}{\lambda}\right)^{\frac{7}{6}} \int_0^R \left(\frac{h}{R}\right)^{\frac{5}{6}} (R-h)^{\frac{5}{6}} C_n^2(h)\,dh \qquad (2\text{-}12)$$

where

$\lambda$     =     wavelength (m)

$R$     =     range or transmission distance (m)

$h$     =     height (m)

Since this variance is for a point receiver, Hinrichs applies an aperture-averaging factor (which will be discussed in the next section using Andrew's model) to get an averaged variance for a finite aperture $\sigma_{\chi\,avg}^2$. Hinrichs then utilizes $\sigma_{\chi\,avg}^2$ to determine the additional margin, *FM*, required to overcome the scintillation effects. For the communications link margin an expectance approach is utilized. This approach differs from an exceedance approach which would be utilized for acquisition link margins (22:1-3; 31:I.10-I.16). Hinrichs states that :

> These approaches differ fundamentally in that in the exceedance approach, the margin is assumed to be sufficient to overcome a fade depth of a given probability. Whereas, the goal in the expectance approach is to design a system which, on the average, meets a certain performance level....The required signal for an acquisition link is based on the probability of detection and false alarm rate which is a single pulse statistic. Therefore, the exceedance approach is used. Whereas, the required signal for a communication link is based on bit error rate which is the average probability of error. Consequently, an expectation approach is used. (22:I.13-I.14)

Hinrichs derives two equations to relate the probability of fade, $P_F$, (for acquisition) and average probability of error, $\overline{P}_e$, (for communications) to the averaged variance, $\sigma_{\chi\,avg}^2$ (22:1-3; 31:I.10-I.16):

$$P_F = Q\left(\frac{\dfrac{-F}{20\log_{10}e + \sigma^2_{\chi avg}}}{\sigma_{\chi avg}}\right) \qquad (2\text{-}13)$$

$$\overline{P}_e = \int_0^\infty \frac{b\exp\left[-a\alpha\lambda_s\right]}{\sqrt{8\pi}\sigma_{\chi avg}\alpha}\exp\left[\frac{-\left(\ln\alpha + 2\sigma^2_{\chi avg}\right)^2}{8\sigma^2_{\chi avg}}\right]d\alpha \qquad (2\text{-}14)$$

where

$P_F$ = probability of fade

$F$ = fade or exceedance margin

$Q(*)$ = gaussian exceedance function $= \dfrac{1}{2}\left(1 - erf\left(\dfrac{*}{\sqrt{2}}\right)\right)$

$\overline{P}_e$ = average probability of error = BER

$a$ = arbitrary constant = 1

$b$ = arbitrary performance parameter = 0.5

$\lambda_s$ = independent variable

$\alpha$ = multiplicative fading parameter

**Aperture Averaging.** The variance of the scintillating signal, $\sigma^2_\chi$, discussed above is for a point source receiver. The variance of this signal can be reduced by averaging over a finite aperture. The amount of reduction depends on the aperture averaging factor which is defined as "...the ratio of the variance of irradiance obtained from a finite size collecting aperture to the corresponding quantity obtained from a point aperture" (55:1608).

2-14

The aperture averaging factor will be applied directly to the scintillation signal variance to reduce the overall atmospheric losses due to scintillation (1:598; 5:1982-1994; 19:169-175; 20:175-180; 21:181-185; 22:1-3; 23:162-165; 31:I.2-I.4; 48:831-837; 52:6.6-6.24; 55:1608-1609). However, since there is no appreciable aperture-averaging effect for upward propagation (uplink: ground-to-satellite), aperture averaging will only apply to the downlink (satellite-to-ground) (55:1608). Andrews applies an aperture-averaging factor $A$ to the point receiver variance, $\sigma_\chi^2$, to get the average variance, $\sigma_{\chi\,avg}^2$, for a finite aperture (1:597-600):

$$\sigma_{\chi avg}^2 = \sigma_\chi^2 A \tag{2-15}$$

where

$$A = 1 + 1.711B - 0.040B^2 - 2.257B^{\frac{5}{6}} \tag{2-16}$$

and

$$B = \frac{kD^2}{4R} \tag{2-17}$$

$k$   =   wavenumber $(cm^{-1}) = \dfrac{2\pi}{\lambda}$

$D$   =   diameter of the receiver aperture (m)

$R$   =   distance traveled through atmosphere (m)

Once the averaged variance is determined, Hinrichs' equations can be utilized to compute the additional margin required to overcome the scintillation losses ($FM$ in the link equation) (22:1-3; 31:I.10-I.16). This fade margin, $FM$, can be plotted against the probability of fade/error ($P_F$ / $P_e$) and the scintillation variance. Figures 2.5 and 2.6 illustrate these relationships.

2-15
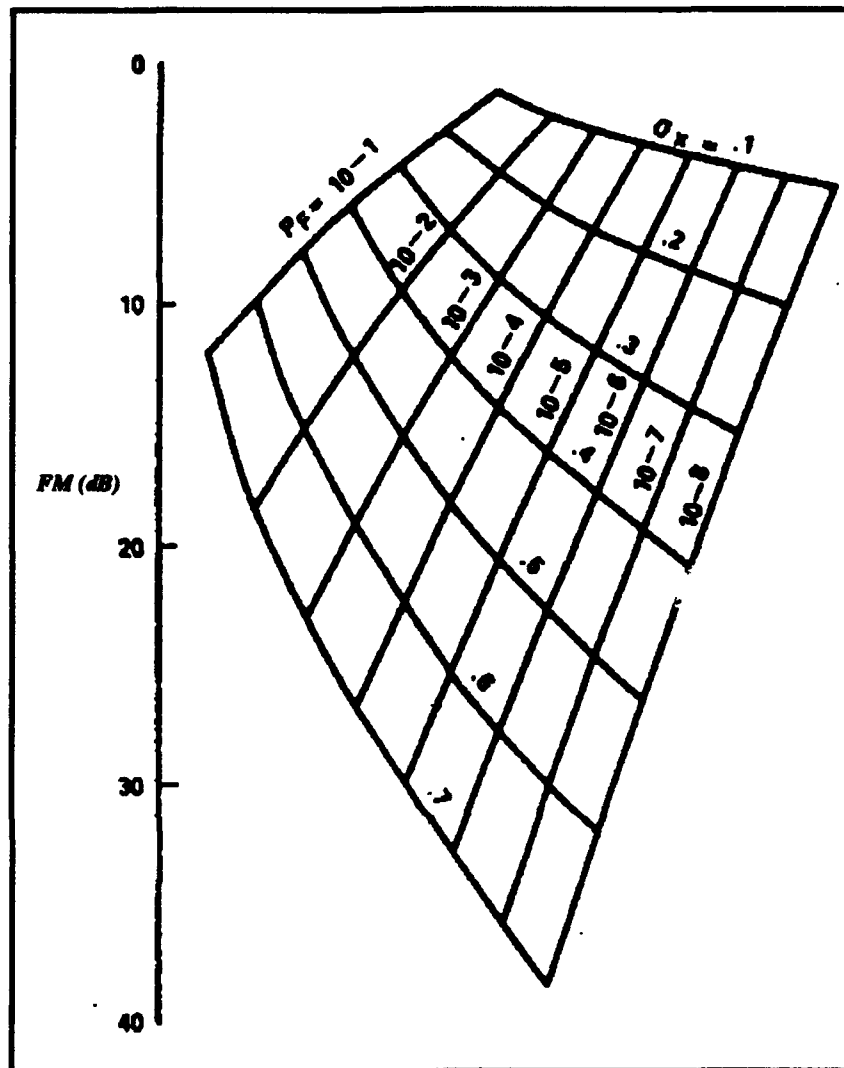
**Figure 2.5 Fade Margin for Acquisition Link (31:I.13)**
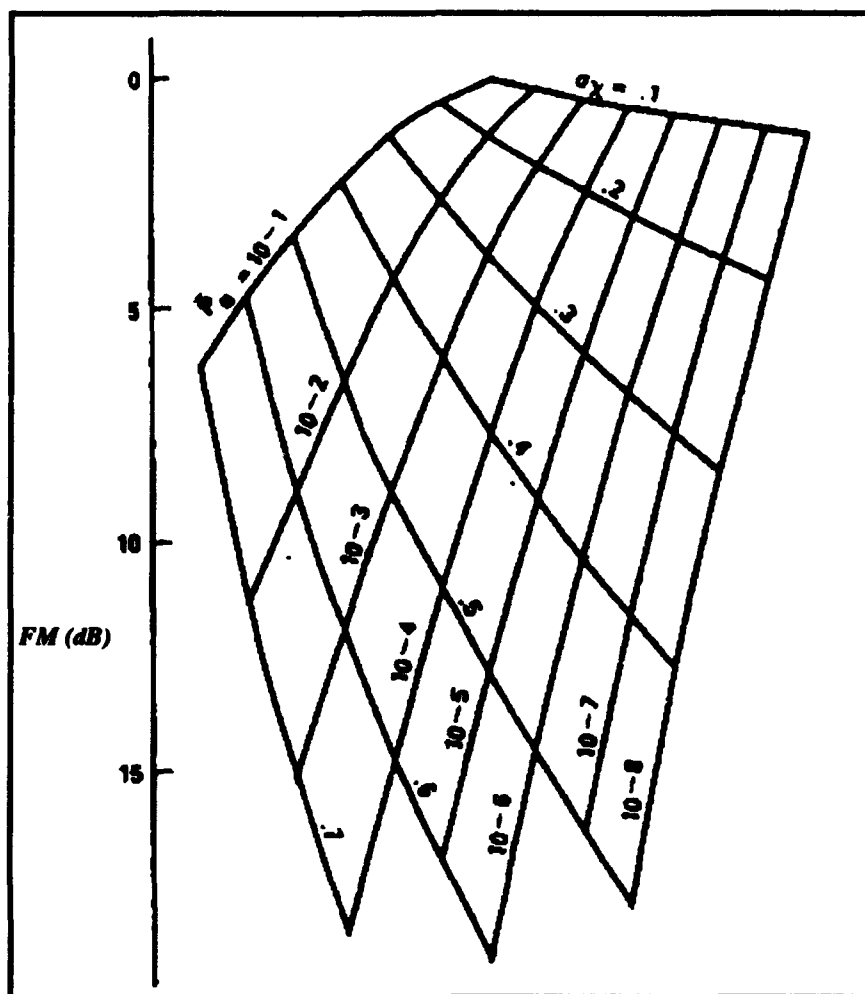
**Figure 2.6  Fade Margin for Communications Link  (31:I.14)**

# Receiver

**Receiver Antenna Gain.** For incoherent receivers, the antenna is an energy collector composed of optics and a detector. The optics focus the incoming energy (photons) down to a spot on the detector. The detector turns this energy into electrical current. The detector is generally much larger than the focus spot, and thus the receiver is generally not sensitive to wavefront aberration. And since the ranges involved for a space-to-ground lasercom system are much, much greater than 5 km (at least 36,000 km for ground-to-geosynchronous), we can assume the wavefront received at the antenna is

virtually a plane wave of flat phase and uniform amplitude distribution (28:27). Receiver gain $G_R$ can be calculated by using the antenna aperture radius, $a$, and the wavelength, $\lambda$ (28:27):

$$G_R = 10 \log_{10}(\frac{2\pi a}{\lambda})^2 \qquad (2\text{-}18)$$

**Receiver Antenna Optics Transmissivity.** The receiver optics are composed of filters, lenses (or mirrors), and other optical elements which all contribute to the overall receiver system transmissivity. The transmissivity of the receiver antenna optics is calculated much the same as the transmit optics transmissivity: individual optical element transmissivities are multiplied together to get a total receiver system transmissivity, $\tau_{rxopt}$.

**Direct Detection Receiver Efficiency.** The receiver efficiency for direct detection, $\eta_{dd}$, is a function of the power falling on the detector (directly related to the projected spot size on the detector) versus the total power received by the system. Figure 2-7 graphs $\eta_{dd}$ versus a plotting parameter $\sigma_d$. (30:2398; 18)

$$\sigma_d = \frac{aR_d}{\lambda f_{eff}} \qquad (2\text{-}19)$$

where $R_d$ is the detector radius, $f_{eff}$ is the effective focal length of the receiver optics, and the plotting parameter $\sigma_d$ represents the ratio of the detector radius to the spot radius.
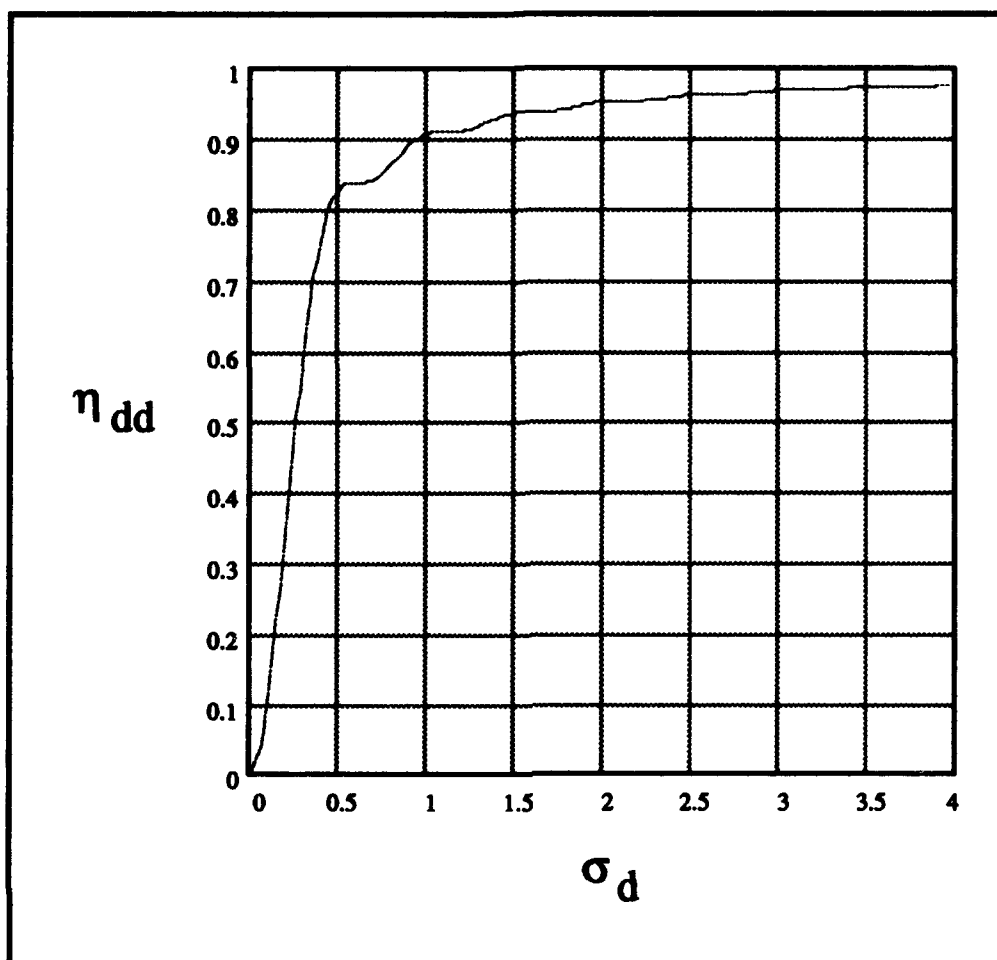
**Figure 2.7 Direct Detection Receiver Efficiency**

**Required Signal.** The required signal, $S_{req}$, for the communications link can be determined by utilizing a given bit error rate (*BER*) and the signal-to-noise ratio *SNR*. The *BER* can be expressed in terms of the error function and the *SNR* (27:22.6):

$$BER = \frac{1}{2}\left[1 - erf\left(\frac{\sqrt{SNR}}{2}\right)\right] \qquad (2\text{-}20)$$

A graphical depiction of the *BER* to *SNR* relationship can be seen in Figure 2-8.

2-19

1

0.1

0.01

0.001

BER     $1 \cdot 10^{-4}$

$1 \cdot 10^{-5}$

$1 \cdot 10^{-6}$

$1 \cdot 10^{-7}$

$1 \cdot 10^{-8}$

0      10      20      30      40      50      60

SNR
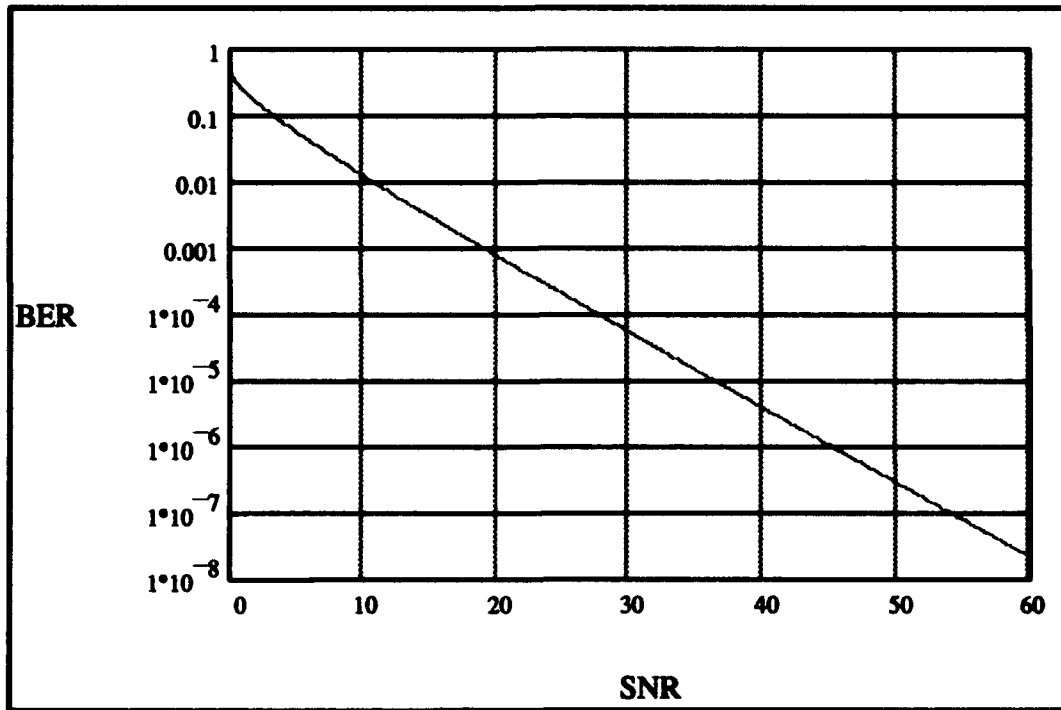
**Figure 2.8  BER versus SNR**

Once the *SNR* from Figure 2-8 is determined from the required *BER*, the required signal, $S_{req}$, can be computed utilizing the mean square signal current $i_{sig}^2$ from the following relationship:

$$SNR = \frac{i_{sig}^2}{i_{sn}^2 + i_{th}^2 + i_{bk}^2 + i_{dk}^2} \qquad (2\text{-}21)$$

where

$i_{sig}^2$  =  mean square signal current (related to $S_{req}$ in the next section)

$i_{sn}^2$  =  mean square shot noise current

$i_{th}^2$  =  mean square thermal noise current

$i_{bk}^2$  =  mean square background noise current

$i_{dk}^2$  =  mean square dark noise current

Each of these terms will be discussed in the sections to follow.

**Signal Current.** The signal current is a function of the arrival of signal photons, the detector efficiency, and the detector gain (2:131):

$$i_{sig} = \frac{q\eta_d P_{sig} \lambda G}{hc} = \frac{q\overline{N}G}{T} \qquad (2\text{-}22)$$

and

$$S_{req} = 10\log_{10}(P_{sig}) \qquad (2\text{-}23)$$

where

$q$ = charge of an electron $(1.602 \times 10^{-19}$ coulombs)

$\eta_d$ = detector quantum efficiency

$P_{sig}$ = signal power received at the detector (watts)

$\lambda$ = signal wavelength (m)

$G$ = detector gain

$h$ = Planck's constant $(6.6254 \times 10^{-34})$

$c$ = speed of light $(3 \times 10^9$ m/sec)

$\overline{N}$ = average number of photoelectrons from signal

$T$ = detector integration time period (sec)

**Shot Noise.** The random arrival of signal photons based on a Poisson distribution cause fluctuations in the detector electrical signal. These fluctuations, in turn, cause a noise in the detector called shot noise. The shot-noise current can be expressed as (2:134; 26:18; 50:258):

$$i_{sn}^2 = \frac{2\eta_d q^2 P_{sig}(BW)G^2\lambda}{hc} = 2qP_{sig}(RS)(BW)G \qquad (2\text{-}24)$$

where

$BW$ = electrical bandwidth $\left(\dfrac{1}{2T}\right)$

$$RS \quad = \quad \text{detector responsivity} = \frac{G\eta_d q\lambda}{hc}$$

**Thermal Noise.** The temperature of a detector gives rise to thermal agitation of electrons and, thus, a current associated with this electron motion. This phenomena is commonly called Johnson noise or Nyquist noise. Thermal noise can be reduced by cooling the detector. Thermal noise can be expressed as (54:323; 50:244):

$$i_{th}^2 = \frac{4kT_{det}(BW)F}{R_d} \tag{2-25}$$

where

$k \quad = \quad$ Boltzman's constant ($1.38 \times 10^{-23}$ j/K)

$T_{det} \quad = \quad$ detector temperature

$R_d \quad = \quad$ detector resistance

$F \quad = \quad$ noise factor

**Background Noise.** The arrival of the background signal photons causes noise just as the arrival of the signal photons do. This background signal, $P_{sig}$, can be determined based on the radiance values (from LOWTRAN7) of the background in the field-of-view (FOV) of the detector. The background noise thus becomes (2:134; 26:17):

$$i_{bk}^2 = \frac{2\eta_d q^2 P_{bk}(BW)G^2\lambda}{hc} = 2qP_{bk}(RS)(BW)G \tag{2-26}$$

**Dark Current Noise.** Inherent in any detector is the noise associated with the current which flows regardless of photons striking the detector. This current is called dark current, $I_{dk}$, and is usually specified by the detector manufacture. The dark current noise, $i^2_{dk}$, becomes (26:18):

$$i^2_{dk} = 2qI_{dk}(BW)G^2 \qquad (2\text{-}27)$$

# III. Results

## System Description

**RF Baseline.** Currently, there are several portable satellite terminals in use by the Department of Defense. The Motorola LST-5C is one of these terminals. Appendix A analyzes the LST-5C and, for purposes of this thesis, the LST-5C will be the RF baseline. The LST-5C gives the user the capability to talk in plain or ciphered voice, or to transmit and receive data. It operates between 2 and 18 watts at 225 - 400 MHz, with either 5- or 25-kHz channel spacing. The entire unit weighs only 11.6 lbs (including the 3.2 lb battery), and fits into any 3.75 x 6 x 9.3 inch space (35:1). It utilizes portable antennas such as the 1-m diameter Trivec Avant AV 2055 antenna which can fold up into a 3.8 x 8 inch case (47:1). A FLTSATCOM geosynchronous satellite was utilized for the satellite end of the link analysis.

For comparison to the lasercom baseline system, here is a summary of the RF baseline parameters:

- BER of $10^{-3}$
- Data Rate of 1200 and 2400 bps
- Output Power of 2 and 18 W
- Antenna Beamwidth of 65 degrees
- System Weight of 11.6 lbs

**Lasercom Baseline.** The system has two terminals: 1) the ground terminal; 2) the geosynchronous (GEO) satellite terminal. Both terminals take advantage of some of the components which McDonnell Douglas designed for their lasercom satellite crosslinks.

Effects of new advances such as the Master Oscillator Power Amplifier (MOPA) will be introduced as variations of the baseline and will be discussed in later sections.

The primary system design specification is to achieve a 1 Gbps link at a $10^{-6}$ BER on both the uplink and downlink, with as little system power consumption and weight as possible. This link will be over a 38,600 km range: ground (northern United States) to geosynchronous orbit.

**Ground Terminal.** The heart of the ground terminal is a six-inch telescope ($f_{eff}$ of 7.4 m for communications link) with a 500-mW multiple-diode-laser (MDL) combiner. The MDL uses six 150-mW AlGaAs laser diodes (SDL 5420 series), operating at 120 mW (reduced power for longer system life: 20+ years ), at a combiner efficiency of approximately 70 percent (6 x 120 mW x 0.70 $\cong$ 500 mW) (46:34-39). Each laser diode operating wavelength is tuned to allow a 10-angstrom diode-to-diode wavelength spacing for dichroic combining. This allows a 50-angstrom bandpass in the 810 to 860 nm operating region of the AlGaAS devices. Wavelength tuning can be accomplished via diode temperature or drive current. The MDL (sixth generation) uses diode temperature, which involves a hermetically-sealed package, a Laser-Diode Package (LDP). (12:1167-1168; 25:7)

Table 3.1 shows the ground terminal parameters for weight and power consumption. The McDonnell Douglas figures reflect a current LEO satellite terminal design which utilizes gimbals and other moving parts which will not be a part of the ground terminal design (12:1169). The ground terminal figures reflect estimates based on reduced system components (moving parts and combined apparatus); the estimated items are ** annotated.

## Table 3.1 Ground Terminal

| Component | McDonnell Douglas LEO Weight (lbs) | Power (W) | Ground Terminal Weight (lbs) | Power (W) |
|---|---|---|---|---|
| Optical Unit (OU) | | | | |
|   Telescope* | 59.2 | 76 | - - - | - - - |
|   Laser Source | 1.2 | 9 | 1.2 | 9 |
|   Detectors/Mechanism | 3.8 | 5 | 3.8 | 5 |
|   Power/Interface Module | 7 | 38.8 | 4** | 2** |
|   6 Inch Optics | 6.8 | - - - | 6.8 | - - - |
|   Bench* | 12.8 | - - - | - - - | - - - |
|   Housing (combines * items) | - - - | - - - | 10** | 2** |
| | | | | |
| Electronics Unit (EU) | | | | |
|   Processor Module | 3.9 | 31.8 | 2** | 2** |
|   Power Control | 4.5 | 11 | - - - | - - - |
|   Optical Unit I/F & Power | 10.8 | 41.1 | 1** | 1** |
| | | | | |
| Cables | 30 | - - - | 0.5** | - - - |
| | | | | |
| Total Weight | 140 | | 29.3 | |
| Total Power | | 212.7 | | 21 |

** Estimated

Ground terminal coarse pointing and tracking is assumed to be accomplished manually and will utilize positioning data and optimum beamwidth for atmospheric beamsteering effects discussed in the previous section. Positioning data could possibly be GPS position data passed between the two terminals as part of the acquisition data stream and periodically as part of the overhead communications data stream. The signal strength can also serve as pointing guidance information. A quad-detector, such as the EG&G C30927E can be used for this purpose.

The terminal mechanism has the capability to "spoil" or widen the beamwidth to 50 mrad for pointing acquisition and tracking. After the link has been established, the beamwidth can be reduced to a narrow beam suitable for a communications link. The narrower beam provides higher power density which allows high data rates, but is wide

enough to allow for atmospheric beamsteering. The communication beamwidth for the uplink baseline will be 26.5 $\mu$rad to allow for atmospheric beamsteering.

The baseline system utilizes a 1 Gbps data link with $10^{-6}$ BER. This data rate for an uplink is several orders of magnitude overkill, since most current applications require only voice and other small-order data rates (100s to 1000s of bps). This may be used as a design tradeoff from the baseline system. For now, 1 Gbps will be used for the uplink data rate. The 1-Gbps downlink data rate could, on the other hand, be useful to ground users trying to get maps, photographs, and other intelligence products. In either case, a 1-Gbps data rate does limit transmission times, which creates a desirable decrease in the probability of intercept.

The receiver utilizes an avalanche photo diode (APD), the EG&G C30902S, with a 0.5-mm diameter, a gain of 250, a 0.5 nsec response time, at an efficiency of 77 percent for the direct detection communications link (15:7; 16:1-3). The total optics transmission is 65 percent. Modulation type is Manchester, or bi-phase, level (non-return to zero: NRZ), with 50 percent duty cycle.

**GEO Terminal.** The baseline GEO Terminal utilizes 24-inch optics ($f_{eff}$ of 4 m for communications link) with the same laser source as the ground terminal (500 mW MDL). As with the ground terminal, other laser sources will be discussed as variations to the baseline. The optics have a transmission $\tau$ of 73 percent. Data rates and BER are the same as the ground terminal (1 Gbps; $10^{-6}$ BER). The GEO terminal is utilizing the same laser source, optical unit, and electronic unit as the McDonnell Douglas LEO satellite terminal listed in Table 3.1 (except for the larger optics and telescope). Table 3.2 lists the weight and power parameters of this GEO terminal (* figures are estimated to reflect the larger telescope and optics). The terminal utilizes direct detection with the same APD as the ground terminal. (12:1169)

**Table 3.2  GEO Terminal**

| Component | Weight (lbs) | Power (W) |
|---|---|---|
| Optical Unit (OU) | | |
| Telescope | 95 | 90* |
| Laser Source | 1.2 | 9 |
| Detectors/Mechanism | 3.8 | 5 |
| Power/Interface Module | 7 | 38.8 |
| 24-Inch Optics | 37.5 | - - - |
| Bench | 12.8 | - - - |
| | | |
| Electronics Unit (EU) | | |
| Processor Module | 3.9 | 31.8 |
| Power Control | 4.5 | 11 |
| Optical Unit I/F & Power | 10.8 | 41.1 |
| | | |
| Cables | 30 | - - - |
| | | |
| Total Weight | 206.5 | |
| Total Power | | 226.7 |

*Estimated

## Laser Sources

Several types of lasers were investigated as possible sources for the lasercom system.
These laser types include: high-power AlGaAs CW single-mode lasers; InGaAs CW
single-mode MOPA lasers; AlGaAs pulsed lasers; and AlGaAs/InGaAs linear/stacked
array lasers. Spectra Diode Labs (SDL) has commercially available products in all these
areas and their lasers will be discussed below.

**AlGaAs CW Single-Mode Lasers.**  SDL has several series (5300, 5400, 5600)
of these type of lasers with differences ranging in output power and single-versus dual-
beam outputs. The SDL-5400 series is the laser which both lasercom baselines utilize.
These devices are ideal for dichroic combining due to their small physical size (0.19 in x
0.35 in) and their ability to be wavelength-tuned via temperature or current (46:35-36).

3-5

Additionally, the SDL-5400 series devices can be operated at modulation rates greater than 2 GHz. (46:34). Since these lasers are CW, the maximum peak power per pulse is limited to the CW power of 150 mW per device. (14:5; 46:34-39; 45:192-197)

**InGaAs CW Single-Mode MOPA Lasers.** The SDL-5760 series lasers are capable of 1 W CW single-mode output (46:44). The device includes an internal thermoelectric cooler for temperature control of the wavelength and is larger (2 in x 11 in) than the SDL-5400 series mentioned above (46:44-46). Recent testing has shown that SDL's MOPA devices are capable of modulation rates of 1 GHz (51:1-2). These devices can also be dichroically combined to produce large amounts of output power (7:328-336; 14:5)

**AlGaAs Pulsed Lasers.** The SDL-2200 series lasers are capable of 3 W peak pulse power, with maximum pulse widths of 500 msec, and a maximum duty cycle of 20 percent (46:64-65). The peak power for these devices is very high, but the device's modulation rate would be too slow for a single channel 1 Gbps lasercom system.

**AlGaAs/InGaAs Linear/Stacked Array Lasers.** The SDL-3200 and 6200 series lasers are very promising for peak pulse power. They range from 60 W to 5000 W of peak power (46:70-89). However these arrayed lasers are generally limited to modulation rates in the hundreds of pulses per second, which make them too slow for a 1-Gbps lasercom system (46:86). This limitation of modulation rate is, in part, due to the problem inherent in modulating the large drive currents of between 88 and 125 amps (46:70-89). These drive currents would also preclude use on the ground terminal, since it is limited to a portable battery for a power supply. Additionally, these devices require cooling mechanisms (conductive or liquid cooled) which add additional space requirements and sub-system complexity (46:70-89).

3-6

## Background Radiance

The background radiances for both the uplink and downlink were computed using PCTRAN7. The major input parameters for both links include:

- 1976 U.S. standard atmospheric model

- Multiple scattering

- Solar illumination from 10° zenith angle and 30° azimuth (relative to uplink)

- 30° elevation angle (60° zenith angle) (relative to uplink)

- Rural 23.0 km visibility aerosol model

- Soil and rock background (for downlink)

Figures 3.1 and 3.2 show the results for the uplink and downlink background radiance in the 780 - 860 nm range. For the baseline lasercom systems, an 810 - 860 nm bandpass filter is utilized to reduce the amount of background radiance the receiver sees. Note that the radiance for the downlink (satellite-to-ground) is several times
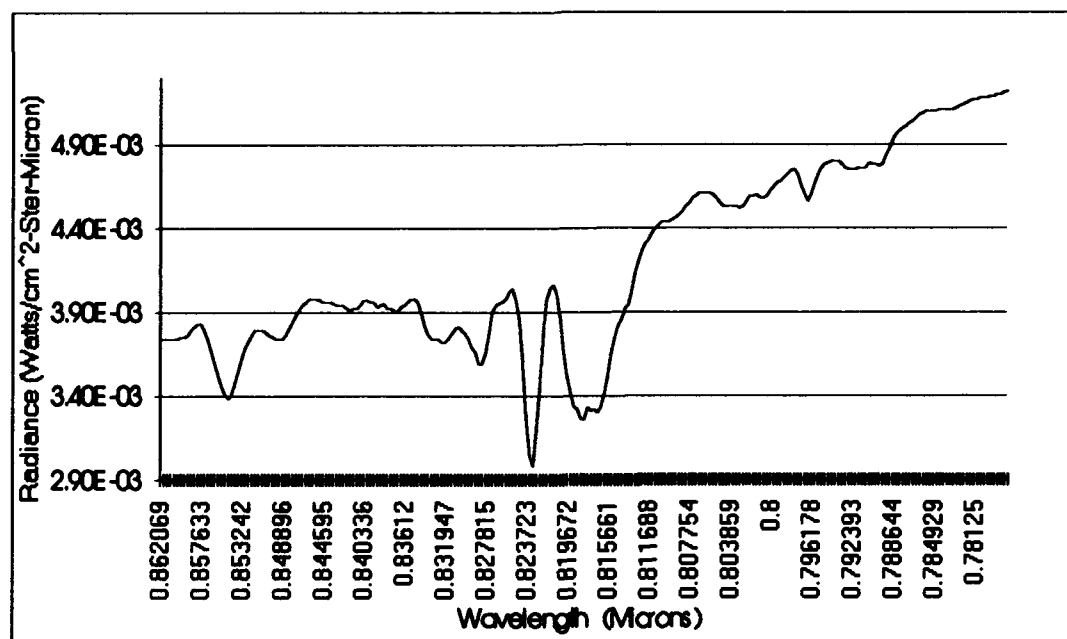


**Figure 3.1 Uplink Background Radiance**

3-7

larger than the uplink (ground-to-satellite). This occurs since additional radiance comes from daytime sun reflecting off the soil and rock background.
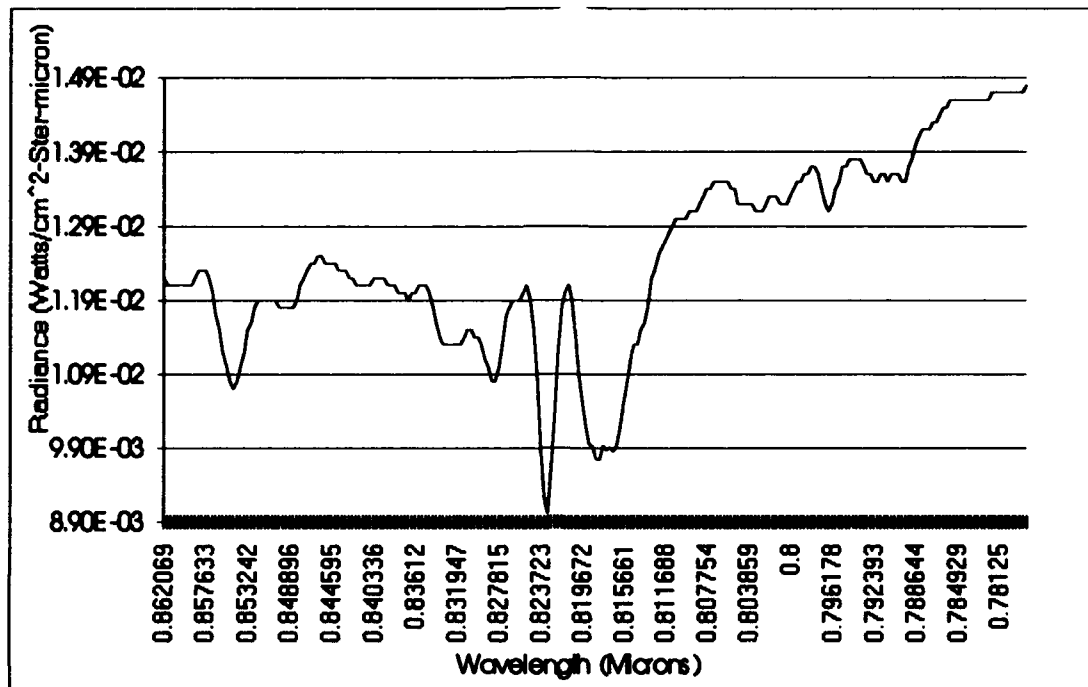


**Figure 3.2 Downlink Background Radiance**

## Atmospheric Transmittance

The atmospheric transmittance for both the uplink and downlink was computed using FASCOD3P. The primary input parameters include:

- All 28 molecular species selected
- Boundary layers at: 0, 1.5, 3.0, 4.5, 6.0, 7.5, 9.0, 10.5, 12.0, 13.5, 15.0, 16.5, 18.0, 19.5, 21.0, 23, 25, 30, 35, 40, 45, 50, 70, 100 km
- 1976 U.S. standard atmospheric model
- 30° elevation angle (60° zenith angle) (relative to uplink)
- Rural 23.0 km visibility aerosol model

These parameters were run for individual laser lines. Atmospheric transmissivity ranged from 63.5 percent for 810 nm to 64.4 percent for 830 nm. There were no major discontinuities (spikes or dips in transmissivity) for the laser lines checked.

## Link Margins

The link margins for both the uplink and downlink were calculated based on the equations presented in the Methodology chapter and the parameters presented in the system description section.

**Uplink.** The uplink is the ground station to geosynchronous satellite link.

**Uplink Baseline.** The uplink baseline computations are summarized in Table 3.3. The link margin shows that the baseline configuration will not work, as it has a -15.0 dB margin. A substantial part of this negative margin comes from the -7 dB fade margin, *FM*, caused by atmospheric scintillation. The 26.5 µrad beamwidth is based

**Table 3.3  Uplink Baseline**

| COMMUNICATIONS - UPLINK Baseline | | |
|---|---|---|
| Laser Peak Power | 500 mw | -3.0 dBW |
| Transmitter Gain (scintillation) | 26.5 µrad | 106.6 dB |
| Transmitter Optics Transmissivity | 0.65 | -1.9 dB |
| Far-Field Efficiency | 0.81 | -0.9 dB |
| Wavefront Efficiency | 0.76 | -1.2 dB |
| Range Loss (FSL) | 38,621 km | -295.3 dB |
| Atmospheric Loss (FASCOD3P) | 0.644 | -1.9 dB |
| Scintillation Margin (FM) | -7 dB | -7 dB |
| Receiver Antenna Gain | 24 inches | 127.3 dB |
| Receiver Optics Transmissivity | 0.73 | -1.4 dB |
| Direct Detection Efficiency | 0.995 | -0.02 dB |
| Received Signal | | -78.8 dBW |
| Required Signal (BER/Noise) | 423.0 nW | -63.7 dBW |
| Margin | | -15.0 dB |

on atmospheric beamsteering effects and, in turn, this beamwidth only allows a 106.6 dB transmitter gain. Several variations to the baseline system could possibly produce a positive margin: laser power, beamwidth, BER, or a combination of these parameters.

**Uplink - High Laser Power.** Increasing the laser power to at least 16 W allows a positive margin for the uplink, as seen in Table 3.4. This would be equivalent to dichroically combining 23 - 1-W MOPA lasers (0.70 x 23 x 1W = 16 W). Although this option is attractive and technically possible, it is not feasible for a portable ground station due to the additional size (each MOPA is 2 in x 11 in) and power requirements (each MOPA requires up to 3.5 A drive current, and 4.0 A of thermoelectric cooler drive current) (46:45-46). However, it may be a feasible option for platforms such as large aircraft which have both the additional space and power supply needed.

Table 3.4 Uplink - High Laser Power

| COMMUNICATIONS - UPLINK 16 W Laser Power | | |
|---|---|---|
| Laser Peak Power | 16000 mw | 12.0 dBW |
| Transmitter Gain (scintillation) | 26.5 urad | 106.6 dB |
| Transmitter Optics Transmissivity | 0.65 | -1.9 dB |
| Far-Field Efficiency | 0.81 | -0.9 dB |
| Wavefront Efficiency | 0.76 | -1.2 dB |
| Range Loss (FSL) | 38,621 km | -295.3 dB |
| Atmospheric Loss (FASCOD3P) | 0.644 | -1.9 dB |
| Scintillation Margin (FM) | -7 dB | -7 dB |
| Receiver Antenna Gain | 24 inches | 127.3 dB |
| Receiver Optics Transmissivity | 0.73 | -1.4 dB |
| Direct Detection Efficiency | 0.995 | -0.02 dB |
| Received Signal | | -63.7 dBW |
| Required Signal (BER/Noise) | 423.0 nW | -63.7 dBW |
| Margin | | 0.01 dB |

**Uplink - Narrow Beamwidth.** Decreasing the beamwidth to at least 4.5 μrad allows enough transmitter gain to give a positive link margin. Table 3.5 shows this margin. Reducing the beamwidth to this size will undoubtedly cause pointing and tracking problems since the atmosphere-induced beamsteering will cause the signal to miss the target satellite occasionally. This beamwidth may be feasible for a system which employs closed-loop fine tracking with gimbaled telescopes at both ends of the loop. However, the portable ground station cannot feasibly utilize a gimbaled telescope due to size, weight, and additional power requirements. Larger platforms such as aircraft, could employ gimbaling techniques. As phased-array lasers become available, they might also be employed to reduce the amount of gimbaling to maintain the fine tracking.

**Table 3.5  Uplink - Narrow Beamwidth**

| COMMUNICATIONS - UPLINK 4.5 μrad Beamwidth | | |
|---|---|---|
| Laser Peak Power | 500 mw | -3.0 dBW |
| Transmitter Gain | 4.5 μrad | 122.0 dB |
| Transmitter Optics Transmissivity | 0.65 | -1.9 dB |
| Far-Field Efficiency | 0.81 | -0.9 dB |
| Wavefront Efficiency | 0.76 | -1.2 dB |
| Range Loss (FSL) | 38,621 km | -295.3 dB |
| Atmospheric Loss (FASCOD3P) | 0.644 | -1.9 dB |
| Scintillation Margin (FM) | -7 dB | -7 dB |
| Receiver Antenna Gain | 24 inches | 127.3 dB |
| Receiver Optics Transmissivity | 0.73 | -1.4 dB |
| Direct Detection Efficiency | 0.995 | -0.02 dB |
| Received Signal | | -63.4 dBW |
| Required Signal (BER/Noise) | 423.0 nW | -63.7 dBW |
| Margin | | 0.4 dB |

**Uplink - Lower BER.** The RF baseline utilizes a BER of $10^{-3}$ and, therefore, a lasercom comparison at this BER should be made. Table 3.6 shows that this BER decreases the negative margin from the baseline's -15.0 dB down to -12.2 dB. This difference comes from the smaller required signal (reduced BER $\Rightarrow$ reduced SNR $\Rightarrow$ reduced required signal).

**Table 3.6 Uplink - Lower BER**

| COMMUNICATIONS - UPLINK BER = 0.001 | | |
|---|---|---|
| Laser Peak Power | 500 mw | -3.0 dBW |
| Transmitter Gain | 26.5 μrad | 106.6 dB |
| Transmitter Optics Transmissivity | 0.65 | -1.9 dB |
| Far-Field Efficiency | 0.81 | -0.9 dB |
| Wavefront Efficiency | 0.76 | -1.2 dB |
| Range Loss (FSL) | 38,621 km | -295.3 dB |
| Atmospheric Loss (FASCOD3P) | 0.644 | -1.9 dB |
| Scintillation Margin (FM) | -7 dB | -7 dB |
| Receiver Antenna Gain | 24 inches | 127.3 dB |
| Receiver Optics Transmissivity | 0.73 | -1.4 dB |
| Direct Detection Efficiency | 0.995 | -0.02 dB |
| Received Signal | | -78.8 dBW |
| Required Signal (BER/Noise) | 217.7 nW | -66.6 dBW |
| Margin | | -12.2 dB |

**Uplink - Lower BER and Narrow Beamwidth.** Combining a lower BER ($10^{-3}$) and at least a 6.5-μrad beamwidth, zeros out the margin. Table 3.7 shows this relationship. The narrower beamwidth makes up most of the margin difference with a 12 dB higher transmitter gain than the baseline. This combination illustrates that the system design has several areas which can be traded off in order to get a link which will work. For the ground terminal, the beamwidth is probably still too narrow to

accommodate coarse pointing and atmospheric beamsteering without some sort of
gimbaling. Again, this configuration would be feasible for larger platforms.

**Table 3.7  Uplink - Lower BER and Narrow Beamwidth**

| COMMUNICATIONS - UPLINK | | |
|---|---|---|
| BER = 0.001 and 6.5 μrad Beamwidth | | |
| Laser Peak Power | 500 mw | -3.01 dBW |
| Transmitter Gain (scintillation) | 6.5 μrad | 118.8 dB |
| Transmitter Optics Transmissivity | 0.65 | -1.9 dB |
| Far-Field Efficiency | 0.81 | -0.9 dB |
| Wavefront Efficiency | 0.76 | -1.2 dB |
| Range Loss (FSL) | 38,621 km | -295.3 dB |
| Atmospheric Loss (FASCOD3P) | 0.644 | -1.9 dB |
| Scintillation Margin (FM) | -7 dB | -7 dB |
| Receiver Antenna Gain | 24 inches | 127.3 dB |
| Receiver Optics Transmissivity | 0.73 | -1.4 dB |
| Direct Detection Efficiency | 0.995 | -0.02 dB |
| Received Signal | | -66.6 dBW |
| Required Signal (BER/Noise) | 217.7 nW | -66.6 dBW |
| Margin | | 0.0 dB |

**Uplink - Lower Data Rate.** A lower data rate variation to the baseline
would appear to be a good system tradeoff. However, since both the baseline laser source
and the MOPA lasers are CW devices, lowering the data rate will not increase the margin.
This occurs because the peak power for a CW device does not change even though the
pulse width increases. Additionally, several other parameters in the margin get worse: the
detector's integration time increases, resulting in an increased noise term and higher
required signal for the same SNR/BER. In short, the transmit power does not increase,
while the required signal does increase. The lower data rate variation would be worth
exploring if the pulsed laser sources were capable of multiple Mpps modulation. Perhaps
in the future, technology for these pulsed laser sources will allow this. The same rationale

applies to the downlink: a lower data rate will not improve the link margin for the baseline laser source or MOPA laser source.

**Downlink.** The downlink is the geosynchronous satellite to ground station link.

**Downlink Baseline.** The downlink baseline computations are summarized in Table 3.8. The link margin shows that the baseline configuration will not work, as it has a -4.3 dB margin. Other than the range loss, *FSL*, the majority of this negative margin comes from the -6 dB fade margin, *FM*, caused by atmospheric scintillation. This occurs since the receiver aperture diameter is only 6 inches, which, in turn, allows a smaller aperture averaging benefit. However, since the transmitter aperture diameter is 24 inches, the beamwidth can be reduced to 8.5 $\mu$rad allowing a 116.5 dB transmitter gain.

**Table 3.8  Downlink - Baseline**

| COMMUNICATIONS - DOWNLINK Baseline | | |
|---|---|---|
| Laser Peak Power | 500 mw | -3.01 dBW |
| Transmitter Gain (scintillation) | 8.5 $\mu$rad | 116.5 dB |
| Transmitter Optics Transmissivity | 0.73 | -1.4 dB |
| Far-Field Efficiency | 0.81 | -0.9 dB |
| Wavefront Efficiency | 0.76 | -1.2 dB |
| Range Loss (FSL) | 38,621 km | -295.3 dB |
| Atmospheric Loss (FASCOD3P) | 0.644 | -1.9 dB |
| Aperture Avg Scint Margin (FM) | -6 dB | -6 dB |
| Receiver Antenna Gain | 24 inches | 127.3 dB |
| Receiver Optics Transmissivity | 0.65 | -1.9 dB |
| Direct Detection Efficiency | 0.995 | -0.02 dB |
| Received Signal | | -68.0 dBW |
| Required Signal (BER/Noise) | 423.0 nW | -63.7 dBW |
| Margin | | -4.3 dB |

**Downlink - High Laser Power.** Increasing the laser power to at least

1.35 W, zeros out the margin. Table 3.9 summarizes this configuration. This variation to

the baseline is entirely feasible for the satellite-based transmitter, since the additional space

requirement, weight requirement, and power consumption of using multiple MOPA lasers

is well within a satellite's capability. McDonnell Douglas has dichroically combined up to

16 laser diodes at up to 75 percent efficiency (13:180; 14:5). Dichroically combining two

1-W MOPA lasers would allow for this increased laser power variation to the baseline (2 x

1 W x 0.75 = 1.5 W).

### Table 3.9  Downlink - High Laser Power

| COMMUNICATIONS - DOWNLINK 1.35 W Laser Power | | |
|---|---|---|
| Laser Peak Power | 1350 mw | 1.3 dBW |
| Transmitter Gain | 8.5 μrad | 116.5 dB |
| Transmitter Optics Transmissivity | 0.73 | -1.4 dB |
| Far-Field Efficiency | 0.81 | -0.9 dB |
| Wavefront Efficiency | 0.76 | -1.2 dB |
| Range Loss (FSL) | 38,621 km | -295.3 dB |
| Atmospheric Loss (FASCOD3P) | 0.644 | -1.9 dB |
| Aperture Avg Scint Margin (FM) | -6 dB | -6 dB |
| Receiver Antenna Gain | 24 inches | 127.3 dB |
| Receiver Optics Transmissivity | 0.65 | -1.9 dB |
| Direct Detection Efficiency | 0.967 | -0.15 dB |
| Received Signal | | -63.7 dBW |
| Required Signal (BER/Noise) | 423.0 nW | -63.7 dBW |
| Margin | | 0.0 dB |

**Downlink - Narrow Beamwidth.** Utilizing a narrower beamwidth of at

least 5.1 μrad also produces a positive margin. Table 3.10 summarizes this variation to

the baseline. Since satellites today should be capable of a pointing jitter of 1 μrad, this

beamwidth should be feasible for a system with closed-loop tracking. However, the limited atmospheric beamsteering (less than the uplink) may cause this beamwidth to be too narrow for continuous communications.

**Table 3.10  Downlink - Narrow Beamwidth**

| COMMUNICATIONS - DOWNLINK 5.1 urad Beamwidth | | |
|---|---|---|
| Laser Peak Power | 500 mw | -3.0 dBW |
| Transmitter Gain | 5.1 urad | 120.9 dB |
| Transmitter Optics Transmissivity | 0.73 | -1.4 dB |
| Far-Field Efficiency | 0.81 | -0.9 dB |
| Wavefront Efficiency | 0.76 | -1.2 dB |
| Range Loss (FSL) | 38,621 km | -295.3 dB |
| Atmospheric Loss (FASCOD3P) | 0.644 | -1.9 dB |
| Aperture Avg Scint Margin (FM) | -6 dB | -6 dB |
| Receiver Antenna Gain | 24 inches | 127.3 dB |
| Receiver Optics Transmissivity | 0.65 | -1.9 dB |
| Direct Detection Efficiency | 0.967 | -0.15 dB |
| Received Signal | | -63.6 dBW |
| Required Signal (BER/Noise) | 423.0 nW | -63.7 dBW |
| Margin | | 0.1 dB |

**Downlink - Lower BER.** As with the uplink, lowering the BER to $10^{-3}$ to match the RF baseline, reduces the negative margin from -4.3 dB (baseline) to -1.4 dB, but does not bring it into the positive range. Table 3.11 summarizes this configuration. As with the uplink, reducing the BER can be utilized for system configuration trade-offs.

**Table 3.11 Downlink - Lower BER**

| COMMUNICATIONS - DOWNLINK BER = 0.001 | | |
|---|---|---|
| Laser Peak Power | 500 mw | -3.0 dBW |
| Transmitter Gain | 8.5 μrad | 116.5 dB |
| Transmitter Optics Transmissivity | 0.73 | -1.4 dB |
| Far-Field Efficiency | 0.81 | -0.9 dB |
| Wavefront Efficiency | 0.76 | -1.2 dB |
| Range Loss (FSL) | 38,621 km | -295.3 dB |
| Atmospheric Loss (FASCOD3P) | 0.644 | -1.9 dB |
| Aperture Avg Scint Margin (FM) | -6 dB | -6 dB |
| Receiver Antenna Gain | 24 inches | 127.3 dB |
| Receiver Optics Transmissivity | 0.65 | -1.9 dB |
| Direct Detection Efficiency | 0.967 | -0.1 dB |
| Received Signal | | -68.0 dBW |
| Required Signal (BER/Noise) | 217.7 nW | -66.6 dBW |
| Margin | | -1.4 dB |

**Downlink - Lower BER and Narrow Beamwidth.** A combination of lowering the BER ($10^{-3}$) and using a narrower beamwidth (7.2 μrad) achieves a positive margin. Table 3.12 summarizes this configuration. Although a 7.2 μrad beamwidth is still narrower than atmospheric beamsteering suggests, it should be within a closed-loop tracking system's capability with current satellite-pointing jitter.

**Downlink - Lower BER and High Laser Power.** Combining both lower BER ($10^{-3}$) and higher laser power (700 mW), zeros out the margin. This variation to the baseline is summarized in Table 3.13. This configuration allows for one 1-W MOPA laser for a single-channel 1 Gbps lasercom system.

**Table 3.12  Downlink - Lower BER and Narrow Beamwidth**

| COMMUNICATIONS - DOWNLINK  BER = 0.001 and 7.2 urad Beamwidth | | |
|---|---|---|
| Laser Peak Power | 500 mw | -3.0 dBW |
| Transmitter Gain | 7.2 urad | 117.9 dB |
| Transmitter Optics Transmissivity | 0.73 | -1.4 dB |
| Far-Field Efficiency | 0.81 | -0.9 dB |
| Wavefront Efficiency | 0.76 | -1.2 dB |
| Range Loss (FSL) | 38,621 km | -295.3 dB |
| Atmospheric Loss (FASCOD3P) | 0.644 | -1.9 dB |
| Aperture Avg Scint Margin (FM) | -6 dB | -6 dB |
| Receiver Antenna Gain | 24 inches | 127.3 dB |
| Receiver Optics Transmissivity | 0.65 | -1.9 dB |
| Direct Detection Efficiency | 0.967 | -0.1 dB |
| | | |
| Received Signal | | -66.6 dBW |
| | | |
| Required Signal (BER/Noise) | 217.7 nW | -66.6 dBW |
| | | |
| Margin | | 0.0 dB |

**Table 3.13  Downlink - Lower BER and High Laser Power**

| COMMUNICATIONS - DOWNLINK  BER = 0.001 and 700 mW Laser Power | | |
|---|---|---|
| Laser Peak Power | 700 mw | -1.5 dBW |
| Transmitter Gain | 8.5 urad | 116.5 dB |
| Transmitter Optics Transmissivity | 0.73 | -1.4 dB |
| Far-Field Efficiency | 0.81 | -0.9 dB |
| Wavefront Efficiency | 0.76 | -1.2 dB |
| Range Loss (FSL) | 38,621 km | -295.3 dB |
| Atmospheric Loss (FASCOD3P) | 0.644 | -1.9 dB |
| Aperture Avg Scint Margin (FM) | -6 dB | -6 dB |
| Receiver Antenna Gain | 24 inches | 127.3 dB |
| Receiver Optics Transmissivity | 0.65 | -1.9 dB |
| Direct Detection Efficiency | 0.967 | -0.1 dB |
| | | |
| Received Signal | | -66.6 dBW |
| | | |
| Required Signal (BER/Noise) | 217.7 nW | -66.6 dBW |
| | | |
| Margin | | 0.0 dB |

# IV. Conclusion

The purpose of this study was to determine if technological advancements have progressed enough to make a man-portable satellite laser communications system feasible. To determine this feasibility three objectives were accomplished: an end-to-end system analysis on the communications link, evaluation of atmospheric effects, and evaluation of semiconductor lasers as the laser source.

## End-to-End Communications Link Analysis

A comparison between a baseline conventional RF satcom system and the baseline lasercom system provided trade-off parameters for analyzing the lasercom uplink and downlink.

**RF versus Lasercom.** The RF baseline currently offers the size, weight, and power consumption compatible with a man-portable system. This RF system is very good for voice and low data rate (1200 and 2400 bps) and all-weather communications. However, the RF beamwidth is so large that jamming and enemy detection are easily accomplished. The RF baseline's size, weight, and low-power consumption provided a benchmark to shoot for on the lasercom baseline. The lasercom baseline could be considered man-portable, but did not meet the same compact and low-power parameters as the RF baseline did. The RF baseline did provide at least one parameter for lasercom system parameter tradeoffs: it operates at a BER of only $10^{-3}$.

The lasercom system offers high-data-rate (1 Gbps), jam-resistant, low-probability-of-detection communications. However, this can only be accomplished via modifications (larger size and power requirements) to the baseline which render the complete lasercom system not man-portable. One half of the system, the downlink, can be modified so that a

man-portable receiver and other larger platforms can be utilized for high-data-rate reception.

**Uplink.** The uplink baseline lasercom system is not feasible due to limitations on portable power supply (battery), aperture size (6-inch diameter), and laser power. These limitations are all imposed by the requirement for the system to be man-portable in a backpack. If technology continues to improve semiconductor lasers and improve batteries to reduce size and weight for more power, this system may be feasible.

Variations to the uplink baseline system are feasible for larger transmitter platforms which are not space, weight, and power supply limited such as large aircraft, ground vehicles, ships, and semi-stationary ground units. These platforms can utilize higher power MOPA devices, gimbaled telescopes, and larger apertures.

**Downlink.** The downlink baseline lasercom system will not work as specified, primarily due to the limitation of the ground receiver aperture size in the link, and the 500-mW transmitter laser power. The transmitter laser power can easily be increased using current MOPA laser technology, which will make a viable transmitter for high-data-rate transmission of photographs, maps, and other high-data-volume information. This variation to the baseline can be used to transmit data to any receiver with a 6-inch aperture or larger: man-portable, ground vehicles, aircraft, ships, and other ground units.

## Atmospheric Effects

Atmospheric effects were a major contributor to the degradation of the system link. Molecular absorption and aerosol scattering caused some degradation in the wavelength regimes utilized, but less than 2 dB loss. Atmospheric scintillation caused the majority of the atmospheric losses. This scintillation loss could be minimized via aperture averaging with more pronounced averaging occurring for larger apertures. The atmosphere also

induces beamsteering effects which must be compensated for with a wider transmitter beamwidth, at the expense of transmitter gain.

## Laser Sources

The most promising laser sources appear to be the high-power AlGaAs CW single-mode lasers and the MOPA lasers currently available through vendors such as SDL. The linear and stacked array lasers offer quantum leaps in power, but cannot be modulated fast enough for Gbps systems.

## Recommendations

Three areas of technological improvement will render a man-portable lasercom system feasible:

- Continued improvement in semiconductor laser power.
- Improved detectors with faster response times and lower noise factors.
- Improved battery size and weight versus power capacity.

Two areas for further study are recommended:

- Data coding and its effect on reducing and eliminating scintillation effects.
- Acquisition and tracking links for portable lasercom systems.

# APPENDIX A - RF BASELINE

## MOTOROLA LST-5C

### Introduction

This appendix will evaluate a radio frequency (RF) baseline system (Motorola LST-5C) which is currently in use by United States Department of Defense personnel. The LST-5C gives the user the capability to talk in plain or ciphered voice, or to transmit and receive data. It operates between 2 and 18 watts at 225 - 400 MHz, with either 5- or 25-kHz channel spacing. The entire unit weighs only 11.6 lbs (including the 3.2 lb battery), and fits into any 3.75 x 6 x 9.3 inch space (35:1). It utilizes portable antennas such as the Trivec Avant AV 2055 antenna which can fold up into a 3.8 x 8 inch case (47:1). The following sections will technically assess how the LST-5C does its job, by analyzing: modulation formats, link margins, carrier to noise margins, and bit error rates.

### Modulation

The LST-5C uses several different types of modulation schemes (35:2):

- Amplitude Modulation (AM) - voice, cipher, data, and beacon
- Frequency Modulation (FM) - voice, cipher, data, and beacon
- Binary Phase-Shift Keying (BPSK) - 1.2 kbps data transmission
- Shaped Binary Phase-Shift Keying (SBPSK) - 2.4 kbps data transmission

MIL-STD-188-181 requires that the modulation for 1.2 kbps and 2.4 kbps data rates be interoperable with BPSK and 50-percent SBPSK modulation formats (33:15). BPSK works well with two-level digital baseband signals. The BPSK carrier has a phase of 90

A-1

degrees for a "1" level and a phase of -90 degrees for a "0" level. Figure 1 shows the BPSK waveform. MIL-STD-188-181 describes the disadvantages of BPSK:

> The disadvantage of BPSK is that it is not spectrally efficient. The abrupt change in phase causes energy to spill over into adjacent channels. This adjacent channel interference (ACI) degrades the communications of other satellite users. Spectral containment cannot be improved by filtering because post-modulation filtering will create a non-constant envelope. (33:29)

Shaped binary phase-shift keying is a variation of BPSK. It has good spectral containment and is compatible with BPSK. Figure 1 shows the SBPSK waveform. MIL-STD-188-181 describes the advantages and disadvantages of SBPSK:

> The main advantage of SBPSK is that the rate of falloff of the side lobes, as compared to the main lobe, is much greater than for BPSK. Thus, the spectral containment is enhanced....SBPSK is created by premodulation filtering that preserves a constant envelope. SBPSK is compatible with BPSK if the shaping does not exceed approximately 50 percent.
>
> The disadvantage of SBPSK is that the shaping degrades detection efficiency. The loss of detection efficiency for an "integrate and dump" detector is approximately 1 dB with 50-percent shaping. (33:31)
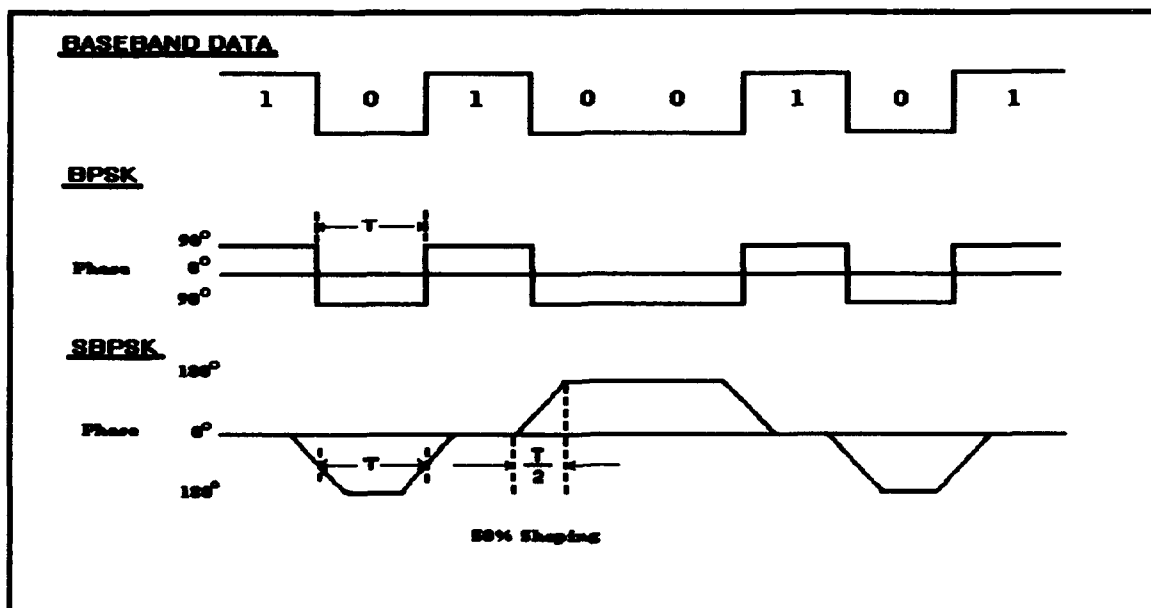


**Figure A.1 Binary Phase Shift Keying (BPSK)** (33:30)

A-2

## Link Margin Analysis

### Power Received

Typically the link margin analysis begins with the computation of how much power actually reaches a receiver from the original transmitted signal. In general, the power received, $P_R$, takes into account: the transmitter power, the antenna gains, and the losses that occur along the way (43:179):

$$[P_R] = [eirp] + [G_R] - [FSL] - [RFL] - [AML] - [AA] - [PL] \qquad \text{(A-1)}$$

where

| | | |
|---|---|---|
| $[P_R]$ | = | received power, dBW |
| $[eirp]$ | = | equivalent isotropic radiated power, dBW |
| $[G_R]$ | = | receiver antenna gain, dB |
| $[FSL]$ | = | free-space loss, dB |
| $[RFL]$ | = | receiver feeder loss, dB |
| $[AML]$ | = | antenna misalignment loss, dB |
| $[AA]$ | = | atmospheric absorption loss, dB |
| $[PL]$ | = | polarization mismatch loss, dB |

Each of these terms will be discussed and calculated in the sections below, followed by a tabulated up/downlink analysis.

### Effective Isotropic Radiative Power

Effective isotropic radiative power *eirp* is "...the product of the power supplied to an antenna and its gain relative to a hypothetical antenna that radiates or receives equally in all directions" (33:5). In decibel form, *eirp* is (43:172):

$$[eirp] = [P_T] + [G_T] \qquad \text{(A-2)}$$

A-3

where

$[P_T]$ = transmitter power, dB

$[G_T]$ = transmitter antenna gain, dB

**Uplink EIRP**

Motorola gives the LST-5C maximum transmitter power for FM as 18 watts (35:2).
Converting this into dBm gives 42.55 dBm. The LST-5C antenna gain, using the Trivec
Avant AV 2055 series antenna is between 7 and 10.5 dB, depending on which model of
the 2055 series antenna used (47:1). Motorola uses 6 dB for a conservative deployable-
site antenna gain and 11 dB for a fixed-site antenna gain (53:1). For comparison
calculations 6 dB and 10.5 dB will be used.

Using 6 dB antenna gain and 42.55 dBm transmitter power gives an [eirp] of 48.55
dBm (Motorola shows 48 dBm). Using 11 dB antenna gain results in an [eirp] of 53.55
dBm (Motorola shows 53 dBm). Using 10.5 dB antenna gain would result in an [eirp] of
53.05 dBm, which is closer to Motorola's figures (53:1).

**Table A.1 Uplink EIRP**

|  | Motorola Deployable Site | Trivec 6-dB Antenna | Motorola Fixed Site | Trivec 10.5-dB Antenna |
|---|---|---|---|---|
| XMTR POWER | -- | 42.55 dBm | -- | 42.55 dBm |
| XMTR ANTENNA GAIN | -- | + 6 dB | -- | + 10.5 dB |
| EIRP | 48 dBm | 48.55 dBm | 53 dBm | 53.05 dBm |

**Downlink EIRP**

Motorola uses a 17-dB gain for their FLTSATCOM satellite antenna. Using
Motorola's *eirp* of 56 dBm, a satellite transmitter power of 39 dBm or 8 watts can be
backed out. This power level per wideband channel seems fairly reasonable for

FLTSATCOM. Both the fixed-site and deployable-site calculations use the 56-dBm

figure. (53:1)

### Table A.2 Downlink EIRP

|  | Motorola Deployable Site | 17-dB Antenna Calculations | Motorola Fixed Site | 17-dB Antenna Calculations |
|---|---|---|---|---|
| XMTR POWER | -- | 39 dBm | -- | 39 dBm |
| XMTR ANTENNA GAIN | -- | ±17 dB | -- | ±17 dB |
| EIRP | 56 dBm | 56 dBm | 56 dBm | 56 dBm |

## Free Space Loss

Free space loss, *FSL*, is the power attenuation of a signal as is spreads out in space. This loss is due to the wave nature of the electromagnetic energy in the RF signal. *FSL* can be calculated by (43:173; 33:37):

$$[FSL] = 32.5 + 20\log f + 20\log d \tag{A-3}$$

where *f* is the frequency in megahertz (MHz) and *d* is the distance in kilometers (km).

The frequency can be determined by going to the band plan for FLTSATCOM. For the uplink and downlink pair of frequencies 300 MHz and 260 MHz will be used (corresponding to Channel Six, the middle of the FM wideband (25 kHz) region band plan in MIL-STD-188-181) (33:45). The distance is 36,000 km for a geosynchronous satellite. The uplink *FSL* comes out to 173.16 dB. The downlink *FSL* comes out to 171.92 dB. Motorola uses 173 dB for both their uplink and downlink calculations, probably for ease of calculation (53:1).

### Table A.3 Free Space Loss

|  | Motorola Uplink | 300-MHz Uplink | Motorola Downlink | 260-MHz Downlink |
|---|---|---|---|---|
| [FSL] | 173 dB | 173.16 dB | 173 dB | 171.92 dB |

## Other Losses

Other losses would include the rest of the right-hand side of Equation 1: receiver feeder loss, *RFL*; antenna misalignment loss, *AML*; atmospheric absorption loss, *AA*; and polarization loss, *PL*. Motorola did not break out these losses in their link-margin analysis. However, Mark Wormley in Motorola's Engineering Customer Support Division, said that they generally use 2 to 3 dB to account for these losses (53:1).

### Receiver Feeder Loss

Motorola takes receiver feeder loss into account with their receiver-sensitivity figure, *RS* (53:1). This means that the minimum-required receiver signal power, *RS*, is measured at the terminals of the antenna. For these calculations, 1.5 dB will be used as an approximate figure for receiver feeder loss.

### Antenna Misalignment Loss

Motorola assumes that the antenna is aligned and that this loss is negligible (53:1). This is probably a reasonable assumption since the antenna has such a wide pattern (3 dB beamwidth is between 65 and 90 degrees, depending on the model antenna) (41:1). Additionally, the LST-5C has a signal-strength meter which enables the user to point the antenna (coarse pointing) to line it up with the strongest signal (53:1). Using the Trivec Avant antenna's 3-dB beamwidth of 65 degrees, the antenna footprint at geosynchronous range would be approximately 32,627 km in diameter (diameter of spot equals the range times the sine of the 3-dB beamwidth: $d_{spot} \cong R\sin\theta_{3dB}$)!

The FLTSATCOM antenna will be assumed to have a very wide 3-dB beamwidth also, so that it can support a wide "footprint" of users on the ground (a 17-degree, 3-dB beamwidth from geosynchronous orbit will cover the earth's hemisphere) (34:86).

**Atmospheric Absorption Loss**

Atmospheric absorption losses occur due to the energy absorption by atmospheric gases. This absorption varies with frequency and primarily affects frequencies centered around 22.3 GHz and 60 GHz. Water vapor causes the absorption at 22.3 GHz and oxygen causes the 60 GHz absorption. From Figure A-2 the atmospheric absorption loss for 300 MHz and 260 MHz is approximately 0.2 dB.



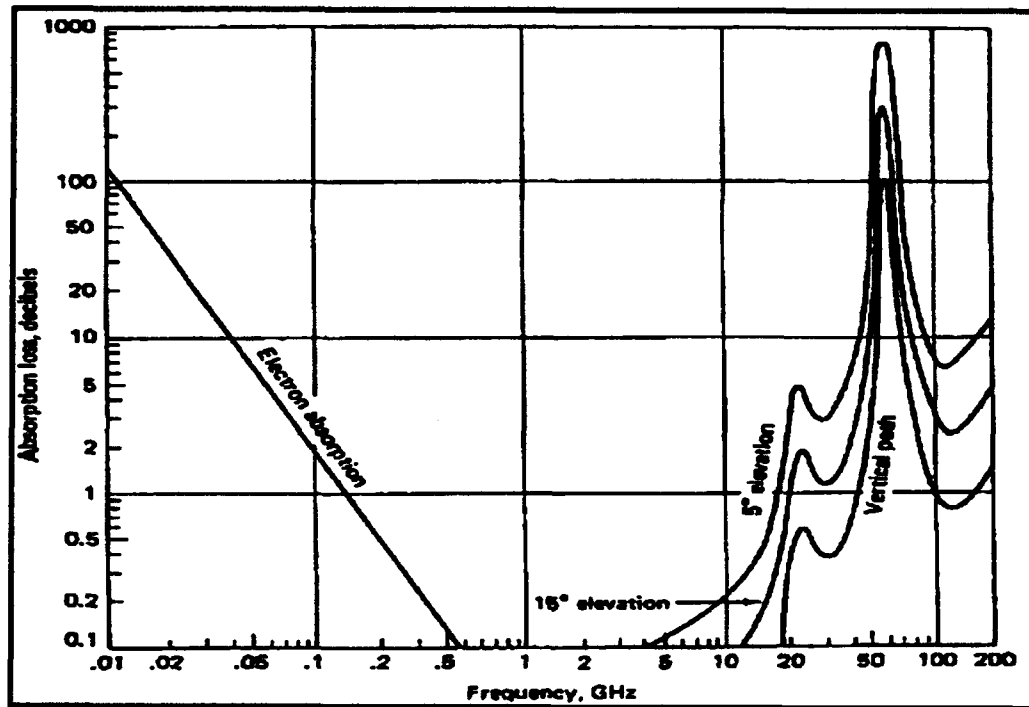**Figure A.2 Atmospheric Absorption Loss (32:113)**

## Fade Margin

Motorola performs their link margin analysis by determining what the fade margin, *FM*, is for both the uplink and the downlink. The fade margin is the difference in decibels between the actual signal power received, $P_R$, and the signal power that the receiver requires (receiver sensitivity, *RS*):

$$[FM] = [P_R] - [RS] \tag{A-4}$$

This figure gives the user an idea of how much additional loss can occur before the signal can no longer be received. Rain is one such loss which is not normally put into the link margin calculations, but will definitely affect performance. Motorola uses the following equation to determine fade margin (53:1):

$$[FM] = [eirp] + [G_R] - [FSL] - [RS] \qquad\qquad (A\text{-}5)$$

Tables A.4 and A.5 show the up/downlink fade margin results using Equation (A-5).

**Table A.4  Uplink Fade Margin**

|  | Motorola Deployable Site | Trivec 6-dB Antenna | Motorola Fixed Site | Trivec 10.5-dB Antenna |
|---|---|---|---|---|
| XMTR POWER | -- | 42.55 dBm | -- | 42.55 dBm |
| XMTR ANTENNA GAIN | -- | + 6 dB | -- | + 10.5 dB |
| EIRP | 48 dBm | 48.55 dBm | 53 dBm | 53.05 dBm |
| FREE SPACE LOSS | -173 dB | -173.16 dB | -173 dB | -173.16 dB |
| RCVR ANTENNA GAIN | 17 dB | 17 dB | 17 dB | 17 dB |
| RCVR SENSITIVITY | + 115 dBm | + 115 dBm | + 115 dBm | + 115 dBm |
| FADE MARGIN | 7 dB | 7.39 dB | 13 dB | 11.89 dB |

**Table A.5  Downlink Fade Margin**

|  | Motorola Deployable Site | Trivec 6-dB Antenna | Motorola Fixed Site | Trivec 10.5-dB Antenna |
|---|---|---|---|---|
| XMTR POWER | -- | 39 dBm | -- | 39 dBm |
| XMTR ANTENNA GAIN | -- | + 17 dB | -- | + 17 dB |
| EIRP | 56 dBm | 56 dBm | 56 dBm | 56 dBm |
| FREE SPACE LOSS | -173 dB | -171.92 dB | -173 dB | -171.92 dB |
| RCVR ANTENNA GAIN | 6 dB | 6 dB | 11 dB | 10.5 dB |
| RCVR SENSITIVITY | + 119 dBm | + 119 dBm | + 119 dBm | + 119 dBm |
| FADE MARGIN | 8 dB | 9.08 dB | 13 dB | 13.58 dB |

## Power Received - Revisited

From Equation (A-4) and the figures for the fade margins in Tables A.4 and A.5, the power received, $P_R$, can be calculated. Tables A.6 and A.7 show the results.

### Table A.6  Uplink Power Received

|  | Motorola Deployable Site | Trivec 6-dB Antenna | Motorola Fixed Site | Trivec 10.5-dB Antenna |
|---|---|---|---|---|
| FADE MARGIN *FM* | 7 dB | 7.39 dB | 13 dB | 11.89 dB |
| RCVR SENSITIVITY *RS* | + -115 dBm | + -115 dBm | + -115 dBm | + -115 dBm |
| POWER RECEIVED *Pₐ* | -108 dBm | -107.67 dBm | -102 dBm | -103.11 dBm |

### Table A.7  Downlink Power Received

|  | Motorola Deployable Site | Trivec 6-dB Antenna | Motorola Fixed Site | Trivec 10.5-dB Antenna |
|---|---|---|---|---|
| FADE MARGIN *FM* | 8 dB | 9.08 dB | 13 dB | 13.58 dB |
| RCVR SENSITIVITY *RS* | + -119 dBm | + -119 dBm | + -119dBm | + -119 dBm |
| POWER RECEIVED *Pₐ* | -111 dBm | -109.92 dBm | -106 dBm | -105.42 dBm |

From Equation (A-1) and the figures from previous sections, the power received, $P_R$, can be calculated and compared to the above figures. Tables A.8 and A.9 show the results of Equation (A-1) and appear to differ from Tables A.6 and A.7 only by the additional 2-dB losses included.

## Carrier to Noise Analysis

### Noise

The major source of noise comes from the random thermal motion of electrons, often called thermal noise. Both the antenna and the receiver pickup this thermal noise and they can be expressed in terms of either a noise factor [$F$] or as a temperature, $T$, in degrees Kelvin (K).

A-9

### Table A.8 Uplink Power Received - Link Equation

|  | Motorola Deployable Site | Trivec 6-dB Antenna | Motorola Fixed Site | Trivec 10.5-dB Antenna |
|---|---|---|---|---|
| [*eirp*] | 48 dBm | 48.55 dBm | 53 dBm | 53.05 dBm |
| [$G_R$] | 17 dB | 17 dB | 17 dB | 17 dB |
| [*FSL*] | -173 dB | -173.16 dB | -173 dB | -173.16 dB |
| [*RFL*] | - | -1.5 dB | - | -1.5 dB |
| [*AML*] | - | 0 dB | - | 0 dB |
| [*AA*] | -2 dB* | -0.2 dB | -2 dB* | -0.2 dB |
| [*PL*] | +    0 dB | +    0 dB | +   0 dB | +    0 dB |
| [$P_R$] | **-110 dBm** | **-109.31 dBm** | **-105 dBm** | **-104.81 dBm** |

\* Estimated sum of [*RFL*], [*AML*], and [*AA*]  from Motorola (53:1)

### Table A.9 Downlink Power Received - Link Equation

|  | Motorola Deployable Site | Trivec 6 dB Antenna | Motorola Fixed Site | Trivec 10.5 dB Antenna |
|---|---|---|---|---|
| [*eirp*] | 56 dBm | 56 dBm | 56 dBm | 56 dBm |
| [$G_R$] | 6 dB | 6 dB | 11 dB | 10.5 dB |
| [*FSL*] | -173 dB | -171.92 dB | -173 dB | -171.92 dB |
| [*RFL*] | - | -1.5 dB | - | -1.5 dB |
| [*AML*] | - | 0 dB | - | 0 dB |
| [*AA*] | -2 dB* | -0.2 dB | -2 dB* | -0.2 dB |
| [*PL*] | +    0 dB | +    0 dB | +   0 dB | +    0 dB |
| [$P_R$] | **-113 dBm** | **-111.62 dBm** | **-108 dBm** | **-107.12 dBm** |

\* Estimated sum of [*RFL*], [*AML*], and [*AA*]  from Motorola (53:1)

The antenna noise, $T_{ant}$, is usually dominated by the *sky noise*, which comes from matter in any form and is present throughout the universe (43:181).  MIL-STD-188-181 uses 200 K as the sky noise (33:33).  However, typical satellite antenna noise temperature

A-10

is 290 K, since it is looking down and receiving the full thermal radiation of the earth. (43:181-183)   Additionally, Figure 3 shows that at 260 MHz  the downlink antenna noise for a LST-5C is approximately 50 K.   For FLTSATCOM (uplink) 290 K will be used as the $T_{ant}$, and 200 K (more restrictive than 50 K) as the $T_{ant}$ for the LST-5C (downlink).

MIL-STD-188-181 states that many current specifications require that the receiver noise figure [F] be 4 dB maximum. (33:33)   Motorola gives the receiver noise figure as
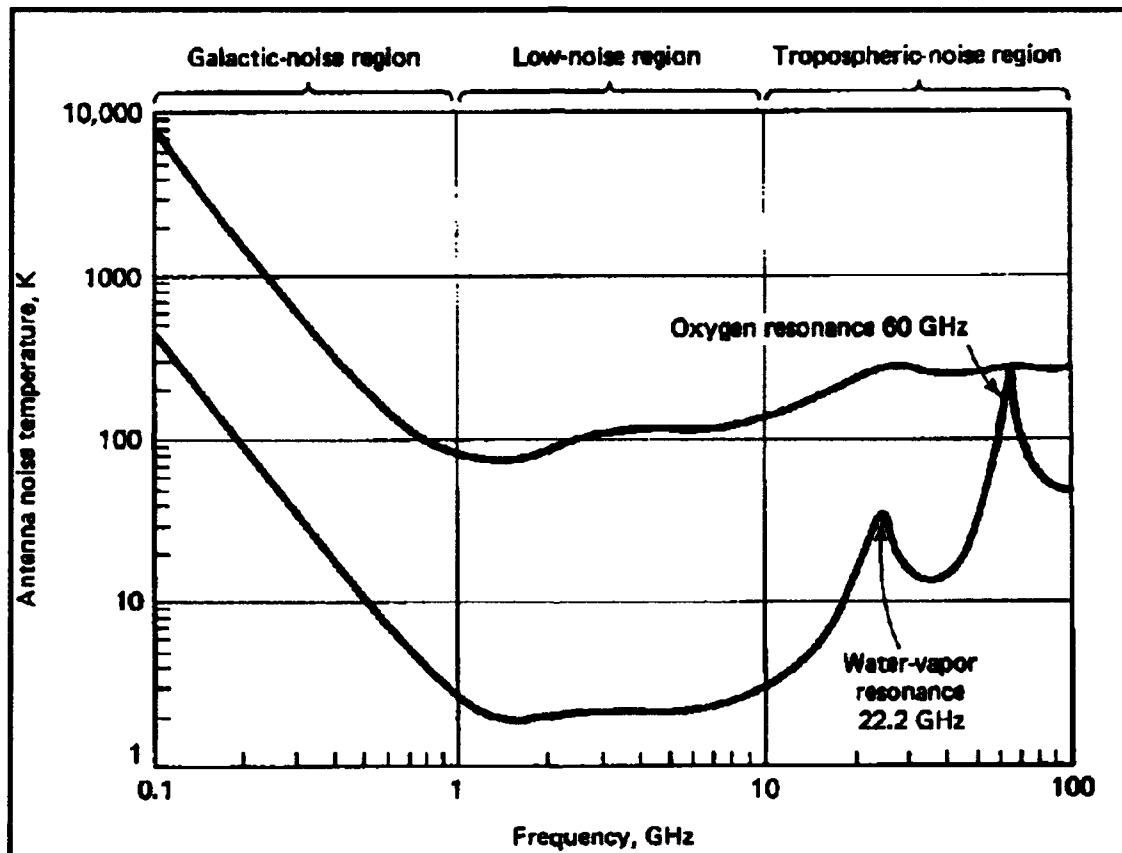


**Figure A.3   Ground Based Antenna Noise**   (43:182)

4-dB, which is consistent with MIL-STD-188-181 (35:2).   Since the actual figure for the FLTSATCOM receiver noise is not available, 4 dB will be used.   From these noise figures the receiver effective temperatures, $T_e$ can be calculated (43:185):

$$[F] = 10 \log F \qquad\qquad (A\text{-}6)$$

$$T_e = (F-1)T_o \qquad\qquad (A\text{-}7)$$

A-11

Where $T_o$ is 290 K, $T_e$ comes out to 438 K. From this figure, we can add the antenna temperature, $T_{ant}$, to the receiver effective temperature, $T_e$, to get the overall system temperature, $T_S$ :

$$T_S = T_{ant} + T_e \qquad \text{(A-8)}$$

$T_S$ comes out to 728 K (28.6 dB) for the FLTSATCOM uplink and 638 K (28 dB) for both the LST-5C downlinks. From here, the receiver-gain-to-noise ratio [$G/T$] for both the uplink and downlink can be calculated with the following equation (43:188):

$$\left[\frac{G}{T}\right] = [G_R] - [T_s] \qquad \text{(A-9)}$$

The uplink [$G/T$] calculates to -22 dB $K^{-1}$ and the downlink [$G/T$] calculates to -11.6 dB $K^{-1}$.

**Uplink Carrier to Noise**

The carrier-to-noise ratio [$C/N_o$] can be calculated using the [$eirp$], [$G/T$], and [$losses$] calculated in previous sections (43:189):

$$\left[\frac{C}{N_o}\right] = [eirp] + \left[\frac{G}{T}\right] - [losses] + 228.6 \qquad \text{(A-10)}$$

Using 175 dB as the approximate overall losses (as listed in Table A.8), the appropriate [$eirp$], and the [$G/T$] ratios calculated above:

$$\left[\frac{C}{N_o}\right]_{UPLINK} = 90 \, \text{dBHz}$$

## Downlink Carrier to Noise

Using 175 dB as the approximate overall losses (as listed in Table A.9), the appropriate [*eirp*], and the [*G/T*] ratios calculated above:

$$\left[\frac{C}{N_o}\right]_{DOWNLINK} = 87.6 \, dBHz$$

## Combined Carrier to Noise

The combined carrier-to-noise ratio [C/No]TOT can be calculated by (43:199):

$$\left[\frac{C}{N_o}\right]_{TOT}^{-1} = \left[\frac{C}{N_o}\right]_{UPLINK}^{-1} + \left[\frac{C}{N_o}\right]_{DOWNLINK}^{-1} \tag{A-11}$$

$$\left[\frac{C}{N_o}\right]_{TOT} = 85.6 \, dBHz$$

## Bit Error Rate Analysis

Bit error rate (BER) is a measure of the probability of errors occurring as the receiver interprets the incoming data (reading a "1" as a "0", and vice-versa). BER is a direct result of the carrier to noise ratio [$C/N_o$] and can be related to both the bit energy to noise ratio [$E_b/N_o$] and the bit rate [$R_b$]. Figure 4 shows the relation between BER and [$E_b/N_o$]. The following equation relates [$C/N_o$], [$E_b/N_o$], and [$R_b$] (43:162; 33:39):

$$\left[\frac{C}{N_o}\right] = \left[\frac{E_b}{N_o}\right] + [R_b] \tag{A-12}$$

Motorola claims a BER of $10^{-3}$ or better, for both the 1200 bit rate and the 2400 bit rate (35:2). Using Figure A.4 and Equation (A-12), Motorola's BER can be checked.
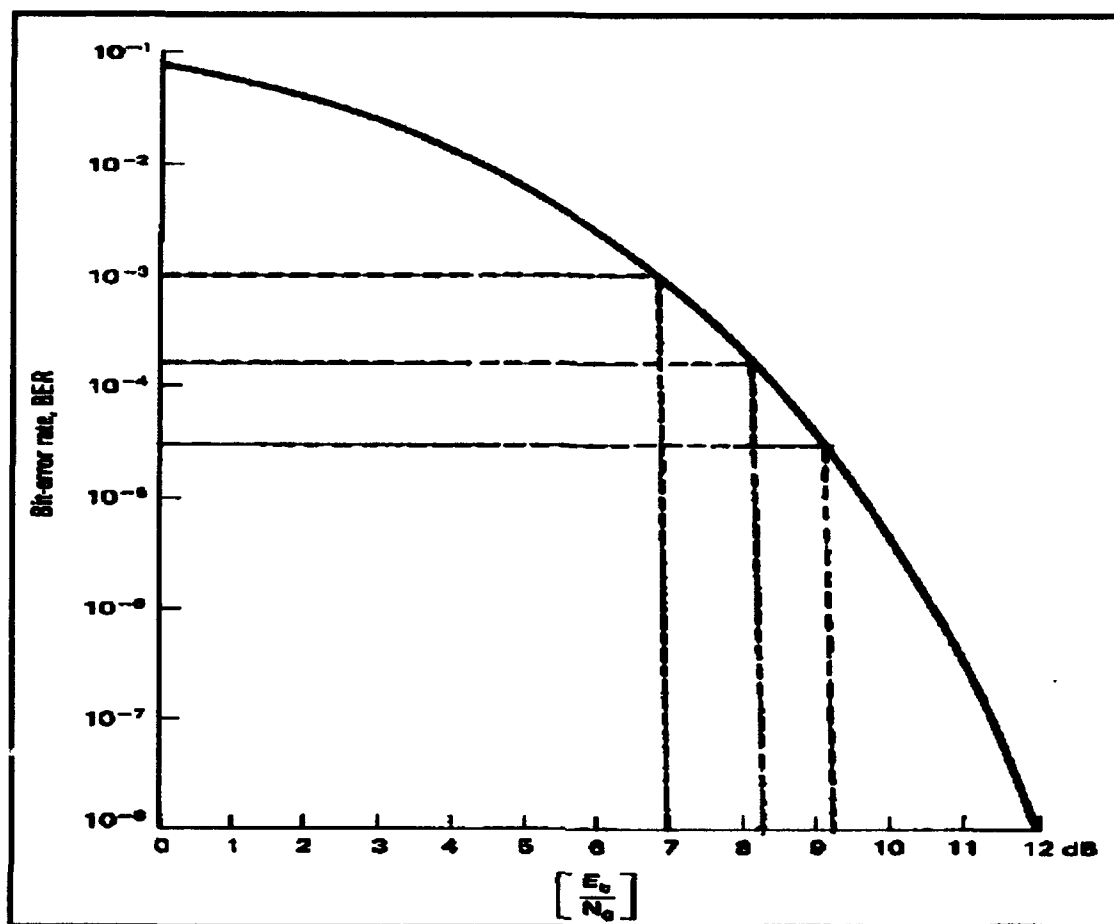
**Figure A.4 Bit Error Rate** (43:142)

## 1200 Bit Rate

At a bit rate of 1200 bps, Motorola claims a $[C/N_o]$ of 39 dB at a $10^{-3}$ BER (35:2). Plugging these numbers into Equation 12 gives us an $[E_b/N_o]$ equal to 8.2 dB. From Figure A.4, an 8.2 dB $[E_b/N_o]$ gives us a BER better than $10^{-3}$ (about 2 x $10^{-4}$), which supports Motorola's claims.

Using Figure A.4 again at $10^{-3}$ BER, gives us a 7 dB $[E_b/N_o]$. Since Motorola has an actual 8.2 dB $[E_b/N_o]$, this gives them a 1.2 dB margin to support their BER (8.2 dB - 7 dB = 1.2 dB).

### 2400 Bit Rate

At a bit rate of 2400 bps, Motorola claims a $[C/N_o]$ of 43 dB at a $10^{-3}$ BER (35:2). Plugging these numbers into Equation (A-12) gives us an $[E_b/N_o]$ equal to 9.2 dB. From Figure A.4, a 9.2 dB $[E_b/N_o]$ gives us a BER better than $10^{-3}$ (about $3 \times 10^{-5}$), which supports Motorola's claims. This also gives Motorola a 2.2 dB margin to support their BER (9.2 dB - 7 dB = 2.2 dB).

## Summary

The LST-5C performs at least as well as Motorola claims. It has a link margin which provides an additional 7 to 13 dB above the receiver sensitivity, for additional losses such as rain or fog. It provides an overall carrier-to-noise ratio of 85.6 dBHz, which should be plenty adequate. And it supports a BER much better than $10^{-3}$. For such a small terminal, it performs remarkably well, and is an asset to military UHF users.

# Bibliography

1. Andrews, L. "Aperture-Averaging Factor for Optical Scintillations of Plane and Spherical Waves in the Atmosphere." *Journal Optical Society of America*, Vol. 9, No. 4: 597-600 (April 1992).

2. Boyd, R. W. *Radiometry and the Detection of Optical Radiation.* New York: Wiley and Sons, 1983.

3. Chetwynd, J. *FASCODE3 Preliminary Version: FASCD3P* (cover letter). U. S. Air Force Geophysics Laboratory, Hanscom AFB MA, 2 Mar 92.

4. Chetwynd, J. Telephone Interviews. U. S. Air Force Geophysics Laboratory, Hanscom AFB MA, Summer/Fall 1993.

5. Churnside, J. "Aperture Averaging of Optical Scintillations in the turbulent Atmosphere." *Applied Optics*, Vol. 30, No. 15: 1982-1984 (20 May 1991).

6. Conner, J. L.; and Fletcher, T. M. "Laser Communication Uplinks and Downlinks," *SPIE High Data Rate Atmospheric and Space Communications,* Boston MA., 996:62-71, 8-9 September 1988.

7. Cornwell, D. "High Power Master Oscillator Power Amplifier (MOPA) AlGaAs Laser for Intersatellite Communications." *SPIE Free-Space Laser Communication Technologies IV,* Los Angeles CA., 1635:328-336, 23-24 January 1992.

8. Davey, K. *Ground-Based Deep-Space LADAR for Satellite Detection: A Parametric Study.* MS thesis, AFIT/GSO/ENS-ENP/89D-1. School of Engineering, Air Force Institute of Technology (AETC), Wright-Patterson AFB OH, December 1986.

9. Deadrick, R.B.; and Deckelman, W. F. "Laser Crosslink Subsystem - An Overview." *SPIE Free-Space Laser Communication Technologies IV,* Los Angeles CA., 1635:225-235, 23-24 January 1992.

10. Dreisewerd, D. Telephone Interviews. McDonnell Douglas Aerospace West, Aerospace Laser Systems and Electronics Division, St. Louis MO, Summer/Fall 1993.

11. Dreisewerd, D. W.; Chenoweth, A. J.; Lambert, S. G.; and Ulrich, G. W. "A GEO to GEO High Data Rate Optical Crosslink Approach." *IEEE MILCOM '92 Proceeding,* San Diego CA., pp. 183-187, 11-14 October 1992.

12. Dreisewerd, D. W.; Lambert, S. G.; Morris, T. R.; and Ulrich, G. W. "A High Data Rate LEO to GEO Optical Crosslink Design." *IEEE MILCOM '92 Proceeding*, San Diego CA , pp. 1163-1169, 11-14 October 1992.

13. Dreisewerd, D. W.; Lambert, S. G.; and Ulrich, G. W. "A Twice Synchronous Range GEO to GEO Optical Intersatellite Link." *IEEE MILCOM '92 Proceeding*, San Diego CA, pp. 177-182 11-14 October 1992.

14. Driemeyer, D. and others. "Size, Weight, and Power Trends in Laser Crosslinks." McDonnell Douglas Technical Services Company, St. Louis MO, 1993

15. EG&G Optoelectronics Canada. *Short Form Catalog - Emitters and Detectors*. EG&G Canada Ltd., Optoelectronics Division, Vaudreuil, Quebec, 1992.

16. EG&G Optoelectronics Canada. *Data Sheet - C30902S*. EG&G Canada Ltd., Optoelectronics Division, Vaudreuil, Quebec, October 1993.

17. EG&G Optoelectronics Canada. *Data Sheet - C30927E*. EG&G Canada Ltd., Optoelectronics Division, Vaudreuil, Quebec, October 1993.

18. Fournier, B. *Design Analysis of a Combined Optical/LADAR Deep-Space Surveillance Satellite*. MS thesis, AFIT/GSO/ENG/93D-01. School of Engineering, Air Force Institute of Technology (AETC), Wright-Patterson AFB OH, December 1993.

19. Fried, D. "Aperture Averaging of Scintillation." *Journal of The Optical Society of America*, Vol. 57, No. 2:169-175 (February 1967)

20. Fried, D. "Propagation of a Spherical Wave in a Turbulent Medium." *Journal of The Optical Society of America*, Vol. 57, No. 2:175-180 (February 1967)

21. Fried, D. and Seidman, J. "Laser-Beam Scintillation in the Atmosphere." *Journal of the Optical Society of America*, Vol. 57, No. 2:181-185 (February 1967)

22. Hinrichs, C. "The Engineering Aspects of Clear Air Laser Propagation." *IEEE MILCOM '85 Proceeding*, Boston MA, pp. 1-5, 20-23 October 1985.

23. Homstad, G. "Aperture-Averaging Effects for Weak Scintillations." *Journal of the Optical Society of America*, Vol. 64, No. 2:162-165 (February 1974)

24. Hufnagel, R. "Variations of Atmospheric Turbulence." *Optical Society of America Topical Meeting on Optical Propagation through Turbulence*, Boulder, CO, July 1974.

25. Jackson, J.; Chenoweth, A.; Dreisewerd, D.; Lambert, S.; and Casey, W. "The Evolution and Future of the Multiple Diode Laser." McDonnell Douglas Aerospace, pp. 1-8, St. Louis MO. (submitted for publication in *SPIE Free-Space Laser Communication Technologies V, 1993*).

26. Jelalian, A. V. *Laser Radar Systems.* Artech House, Norwood, MA, 1992.

27. Jordan, E. C. , ed. *Reference Data for Engineers: Radio, Electronics, Computer, and Communications.* Indianapolis: H. W. Sams and Co., 1985.

28. Katzman, Morris, ed. *Laser Satellite Communication* . Englewood Cliffs: Prentice-Hall, Inc., 1987.

29. Klein, B.; Degnan, J. "Optical Antenna Gain. 1: Transmitting Antennas." *Applied Optics*, 13: 2134-2141 (September 1974).

30. Klein, B.; Degnan, J. "Optical Antenna Gain. 2: Receiving Antennas." *Applied Optics*, 13: 2397-2401 (October 1974).

31. McDonnell Douglas Astronautics. *Appendix I: Atmospherics*, McDonnell Douglas Astronautics Company, pp. I.1-I.33, St. Louis MO.

32. Martin, J. *Communications Satellite Systems*. Englewood Cliffs: Prentice-Hall, Inc., 1978.

33. MIL-STD-188-181. *Interoperability Standard for Dedicated 5-KHz and 25-KHz UHF Satellite Communications Channels*, 1992.

34. Morrow, R. *EENG 421 Class Notes*. U. S. Air Force Institute of Technology, Wright Patterson AFB OH, Fall 1992.

35. Motorola Inc. *LST-5C*. Motorola Inc., Communications Products Office, Scottsdale AZ, 1991.

36. Ontar Corp. *Product/Price Listing* (7 Jul 93 fax from N. Andover sales office). Ontar Corp., Brookline MA, 1993.

37. Ontar Corp./USAF Geophysics Laboratory. *PC-TRAN7*. Ontar Corp., Brookline MA, 1989.

38. Owen, K. *The LOWTRAN7 Atmospheric Transmittance and Radiance Computer Model*. Wright-Patterson AFB OH, 1990.

39. O'shea, D., Callen, W., Rhodes, W. *Introduction to Lasers and Their Applications*. Reading MA:Addison-Wesley, 1977.

40. Pratt, W. K. *Laser Communication Systems*. New York: Wiley and Sons, 1969.

41. Regala, F. Telephone interview and fax transmittal. Trivec-Avant Corp., Huntington Beach CA, May 18, 1993.

42. Roddier, F. "The Effects of Atmospheric Turbulence in Optical Astronomy." *Progress in Optics*, XIX: 341-351 (1979).

43. Roddy, D. *Satellite Communications*. Englewood Cliffs: Prentice-Hall, Inc., 1989.

44. Schmok, S.Telephone interview. Motorola Inc., Government Electronics Group, Scottsdale AZ, April 23, 1993.

45. Scifres,D. et. al. "High Power, High Reliability Laser Diodes." *SPIE Laser Diode Technology and Applications*, Los Angeles CA, 1634:192-197, 20-22 January 1992.

46. Spectra Diode Labs. *1993 Laser Diode Product Catalog*. Spectra Diode Labs, San Jose CA, 1993.

47. Trivec Avant Corp. *AV 2055 SATCOM Antenna*. Trivec Avant Corp., Huntington Beach CA, 1991.

48. Wang, S., Baykal, Y. , and Plonus, M. "Receiver-Aperture Averaging Effects for the Intensity Fluctuation of a Beam Wave in the Turbulent Atmosphere." *Journal of the Optical Society of America*, Vol. 73, No. 6:831-837 (June 1983)

49. Weaver, S. Personal Interviews and Training. Air Force Staff Meteorologist, Wright-Patterson AFB OH, Summer/Fall, 1993.

50. Webb, P., McIntyre, R., and Conradi, J., "Properties of Avalanche Photodiodes." *RCA Review*, 35:234-278 (June 1974)

51. Welch, D. F. *Modulation Characteristics of the SDL MFA-MOPA*. Spectra Diode Labs, San Jose Ca, September 1993.

52. Wolfe, W. and Zissis, G. Eds. *The Infrared Handbook*. Office of Naval Research, Department of the Navy, Washington DC, 1978.

53. Wormley, M. Telephone interview and fax transmittal. Motorola Inc., Engineering Customer Support, Scottsdale AZ, April -May 1993.

54. Yariv, A. *Introduction to Optical Electronics*. New York: Holt, Rinehart, and Winston, 1976.

55. Yura, H. and McKinley W. "Aperture Averaging of Scintillation for Space-to-Ground Optical Communication Applications." *Applied Optics*, Vol. 22, No. 11: 1608-1609 (1 June 1983)

# Vita

Major Brian C. Page was born on 14 March 1957 in St. Louis, Missouri. He graduated from Evergreen High School in Evergreen, Colorado in 1975 and attended the U. S. Air Force Academy, graduating with a Bachelor of Science in Engineering Sciences (specialty: Electrical Engineering) in May 1979. Upon graduation, he successfully completed Undergraduate Pilot Training (Helicopters) at Fort Rucker, Alabama. His first flying assignment was at Malmstrom AFB, Montana, flying search and rescue missions and missile site support in U/TH-1F helicopters. His second flying tour included piloting combat search and rescue missions at Osan AB, Republic of Korea in C/HH-3 aircraft. A follow-on flying tour at Hickam AFB, Hawaii, allowed him to start work in the test and evaluation acquisition arena, by flying HH-53 aircraft recovering de-orbited space equipment. At Hill AFB, Utah, he flew NCH-53 aircraft for test and evaluation missions including mid-air retrieval of unmanned aerospace vehicles. H.Q. *Air Force System Command* chose him to manage their test pilot and navigator resources, and to work rated policy issues at Andrews AFB, Maryland, prior to entering the Graduate School of Engineering, Air Force Institute of Technology, in May 1992. His follow-on assignment is at the H.Q. U. S. Space Command, Peterson AFB, Colorado.

Permanent Address:

> c/o Mr R. Gantt
> 3225 LaRonda Pl NE
> Albuquerque, NM 87110

# REPORT DOCUMENTATION PAGE

Public reporting burden for this collection of information is estimated to average 1 hour per response, including the time for reviewing instructions, searching existing data sources, gathering and maintaining the data needed, and completing and reviewing the collection of information. Send comments regarding this burden estimate or any other aspect of this collection of information, including suggestions for reducing this burden, to Washington Headquarters Services, Directorate for information Operations and Reports, 1215 Jefferson Davis Highway, Suite 1204, Arlington, VA 22202-4302, and to the Office of Management and Budget, Paperwork Reduction Project (0704-0188), Washington, DC 20503.

| 1. AGENCY USE ONLY (Leave blank) | 2. REPORT DATE December 1993 | 3. REPORT TYPE AND DATES COVERED Master's Thesis |
|---|---|---|

**4. TITLE AND SUBTITLE**
SYSTEM DESIGN ANALYSIS OF A LIGHTWEIGHT LASER SATELLITE TERMINAL

**5. FUNDING NUMBERS**

**6. AUTHOR(S)**
Brian C. Page, Major, USAF

**7. PERFORMING ORGANIZATION NAME(S) AND ADDRESS(ES)**
Air Force Institute of Technology, WPAFB OH 45433-6583

**8. PERFORMING ORGANIZATION REPORT NUMBER**
AFIT/GSO/ENG/93D-03

**9. SPONSORING/MONITORING AGENCY NAME(S) AND ADDRESS(ES)**
N/A

**10. SPONSORING/MONITORING AGENCY REPORT NUMBER**

**11. SUPPLEMENTARY NOTES**

**12a. DISTRIBUTION/AVAILABILITY STATEMENT**
Approved for public release; distribution unlimited

**12b. DISTRIBUTION CODE**

**13. ABSTRACT (Maximum 200 words)**
This study investigated the technological feasibility of a man-portable satellite laser communications system. Areas of interest were: an end-to-end system analysis on the communications link; evaluation of atmospheric effects; and evaluation of semi-conductor lasers as the laser source. A literature search revealed that satellite laser communication research is primarily directed at inter-satellite links. There have been some proposed systems for space-to-ground laser communications systems, but they all utilize large fixed ground stations. The focus of this research effort is directed at a small man-portable ground station capitalizing on recent advances in semiconductor laser devices.

Baseline satellite communication systems were analyzed for both conventional radio frequency systems and a laser communication system. Modifications to the laser communications system were explored, and found to be feasible for some applications. Atmospheric effects were explored and are a major contributor to system degradation. Semiconductor laser sources were evaluated and are currently useful for some satellite laser communication applications.

**14. SUBJECT TERMS**
Laser Communications, Satellite Communications, Optical Communications, Portable Satellite Terminals

**15. NUMBER OF PAGES**
81

**16. PRICE CODE**

| 17. SECURITY CLASSIFICATION OF REPORT | 18. SECURITY CLASSIFICATION OF THIS PAGE | 19. SECURITY CLASSIFICATION OF ABSTRACT | 20. LIMITATION OF ABSTRACT |
|---|---|---|---|
| Unclassified | Unclassified | Unclassified | UL |

NSN 7540-01-280-5500

Standard Form 298 (Rev. 2-89)